

More for less: Predicting and maximizing genetic variant discovery via Bayesian nonparametrics

Lorenzo Masoero* Federico Camerlenghi† Stefano Favaro‡
Tamara Broderick§

Abstract

While the cost of sequencing genomes has decreased dramatically in recent years, this expense often remains non-trivial. Under a fixed budget, then, scientists face a natural trade-off between quantity and quality; they can spend resources to sequence a greater number of genomes (quantity) or spend resources to sequence genomes with increased accuracy (quality). Our goal is to find the optimal allocation of resources between quantity and quality. Optimizing resource allocation promises to reveal as many new variations in the genome as possible, and thus as many new scientific insights as possible. In this paper, we consider the common setting where scientists have already conducted a pilot study to reveal variants in a genome and are contemplating a follow-up study. We introduce a Bayesian non-parametric methodology to predict the number of new variants in the follow-up study based on the pilot study. When experimental conditions are kept constant between the pilot and follow-up, we demonstrate on real data from the gnomAD project that our prediction is more accurate than three recent proposals, and competitive with a more classic proposal. Unlike existing methods, though, our method allows practitioners to change experimental conditions between the pilot and the follow-up. We demonstrate how this distinction allows our method to be used for (i) more realistic predictions and (ii) optimal allocation of a fixed budget between quality and quantity.

1 Introduction

New genomic data promise to reveal more of the diversity, or *variation*, among organisms, and thereby new scientific insights. However, collecting genetic data requires resources, and optimal allocation of these resources is a challenging task. Under a fixed budget constraint, there is often a natural trade-off between quality and quantity in genetic experiments. Sequencing genomes at a higher quality reveals more details

*Department of Electrical Engineering and Computer Science, Massachusetts Institute of Technology, lom@mit.edu

†Department of Economics, Management and Statistics, University of Milano-Bicocca

‡Department of Economic and Social Sciences, Mathematics and Statistics, University of Torino

§Department of Electrical Engineering and Computer Science, Massachusetts Institute of Technology

about individuals' genome but also incurs a higher cost. Conversely, sequencing more genomes reveals more about variation across the population but similarly costs more to accomplish. It is then crucial to understand how to optimally allocate a fixed budget between quality and quantity, in the service of learning as much as possible from an experiment.

To maximize the amount learned from a genetic experiment, it is useful to first precisely quantify a notion of "amount learned." In genomics, scientists typically consider a so-called *reference genome* for a species of interest in the experiment. Then, we say that any difference in an observed genome relative to the reference genome constitutes a (genetic) variant. Variants are known to be important for understanding evolution [Consortium, 2015, Mathieson and Reich, 2017], diversity of organisms [Consortium, 2015, Sirugo et al., 2019], oncology [Chakraborty et al., 2019], and disease [Cirulli and Goldstein, 2010, Zuk et al., 2014, Bomba et al., 2017]. Thus, the number of variants in the genome constitutes a concrete metric of "amount learned" from a genetic experiment. Given such a metric, it remains to use the information from a pilot study, to which scientists have typically access, in order to maximize the number of new variants discovered in a follow-up study. That is, the goal is to maximize the number of variants found in the follow-up that were not already found in the pilot. Since any successful experimental procedure should specify how to best trade off resources between quality and quantity, an intermediate step consists in first predicting the number of new variants in the follow-up study under different allocations of budget with respect to quality and quantity. Then, the optimal allocation of a budget can be determined by choosing the experimental setting that maximizes the number of new variants in the follow-up study.

Predicting the number of new variants observed in a follow-up study relative to a pilot study has a rich history in the statistics and genetics literature. Note that, in the variant formulation, we may think of each organism as belonging to multiple "groups," where each group is defined by a particular variant. And our goal is to discover the number of new groups in a follow-up study. A simpler special case of this formulation occurs when each organism belongs to a single group – such as a species or sub-species [Fisher et al., 1943, Good and Toulmin, 1956, Efron and Thisted, 1976, Burnham and Overton, 1978, Orlitsky et al., 2016]. In the single group-per-organism case, the groups are also sometimes called *elements of a partition* or *clusters* [Lijoi et al., 2007]. Analogously, when organisms – or data points – can belong to multiple groups, as in genetic variation, the groups may be called *elements of a feature allocation* [Broderick et al., 2013, Campbell et al., 2018]. Researchers have developed a wide range of approaches for predicting the amount of genetic variation – or new *features* – in a follow-up study. These approaches include Bayesian methods [Ionita-Laza et al., 2009], jackknife-based estimators [Gravel, 2014], linear programs [Gravel, 2014, Zou et al., 2016], and variations on the Good-Toulmin estimator [Orlitsky et al., 2016, Chakraborty et al., 2019]. To the best of our knowledge, though, none of this existing work – in any of the species sampling, feature allocation, or genetics literatures – provides predictions when the experimental conditions may change between the pilot and follow-up study. And thus none of this existing work can be used directly for optimal allocation of a fixed budget in experimental design. On the other hand, in pioneering work, Ionita-Laza and Laird [2010] propose how to allocate a fixed budget in a *pilot* study. That is, the method of

Ionita-Laza and Laird [2010] applies only when no data has yet been observed. Without preliminary data to learn from, though, every data set is treated the same. We expect a priori that different data sets will exhibit different variation patterns. In these cases, data from the pilot should, and will, play a crucial role in informing how to best design the follow-up.

In the present work, we propose a Bayesian nonparametric methodology to predict the number of new variants to be discovered in a follow-up study given observed data from a pilot study. Critically, our approach works when the experimental conditions change between the pilot and follow-up. We then demonstrate how to apply the proposed methodology for designing a follow-up study given data available from a pilot study. For prediction, we use a classic Bayesian nonparametric framework for feature allocations known as the *beta-Bernoulli process* [Hjort, 1990, Kim, 1999, Thibaux and Jordan, 2007, Teh and Gorur, 2009]. The posterior distributions of all our predicted quantities, such as the number of new variants to be discovered, are available in closed form. Our corresponding Bayesian estimators are simple, computationally efficient, and scalable to massive datasets. In addition, our Bayesian nonparametric framework captures realistic power laws in genetic data. And Bayesian hierarchical modeling allows us to straightforwardly accommodate changes in experimental setup. We will see that, when the pilot and follow-up studies are constrained to have the same experimental setup as in previous work, our Bayesian nonparametric predictions are competitive with the state-of-the-art and superior to a number of recent proposals. Most importantly, though, we demonstrate that our predictions maintain their accuracy when experimental conditions change between the pilot and follow-up. Finally, we give an empirical demonstration of how our predictions can be used for designing the follow-up study with an optimal allocation of a fixed budget between quality and quantity. We validate the proposed methodology on synthetic and real data, with a focus on the recent gnomAD dataset of Karczewski et al. [2019].

2 Data and modelling assumptions

Modern high-throughput sequencing technologies allow accurate determination of an organism’s genome [Reuter et al., 2015]. Typically for some population of interest, researchers define a *reference genome*, which serves as a fixed representative for this population. We say that a *variant* is observed wherever a sequenced genome differs from the reference genome. Variants can take many forms – including deletions, inversions, translocations, and insertions [Taylor and Taylor, 2004]. Throughout the present work, we do not distinguish between different forms of variants, though we briefly discuss how our framework could be extended to make this distinction in Section 7. In particular, we consider the case where the variants in a sample of $N \geq 1$ individuals have already been observed in a pilot study, and we wish to predict the number of new variants that we will observe if we were to take a follow-up sample of size $M \geq 1$. That is, we consider the statistical problem of predicting the number of variants in the follow-up study of size M that were not already observed in the pilot study of size N . We will see that our methods can be extended in a straightforward manner to multiple rounds of studies. To establish notation and start building up to our full Bayesian

nonparametric model, we first assume observation of variants is flawless; we will then consider a more realistic model for variant determination in Section 3.2.

Let N denote the number of organisms whose genomes were sequenced in the pilot study, and suppose there are J variants observed among these genomes, with $0 \leq J < \infty$. Let ψ_j denote a label that distinguishes the j -th variant among other possible variants. We will see that using these labels allows us to consider the index ordering j immaterial, but for concreteness it may be convenient to assume that variants are ordered as they appear in the sample with tie-breaking according to a *lexicographic order* [Campbell et al., 2018]. Let $x_{n,j}$ equal 1 if the variant with label ψ_j is observed for the n -th organism; otherwise, let $x_{n,j}$ equal 0. We collect all the variant information for the n -th organism in the measure $X_n := \sum_{j=1}^J x_{n,j} \delta_{\psi_j}$, which pairs each variant observation with the corresponding variant label by putting a mass of size $x_{n,j}$ at location ψ_j . Throughout the paper we use the notation $X_{N_1:N_2}$, where $N_1 \leq N_2$, to denote the set $\{X_{N_1}, X_{N_1+1}, X_{N_1+2}, \dots, X_{N_2}\}$. Given the observable $X_{1:N}$, we consider a Bayesian approach to predict the number of variants in the follow-up study. Specifically, letting Θ be an appropriate latent parameter, we specify a generative model via a likelihood function $\text{pr}(X_{1:N}|\Theta)$ and a prior distribution $\text{pr}(\Theta)$. Bayes Theorem then yields the posterior distribution $\text{pr}(\Theta|X_{1:N})$ and the predictive distribution $\text{pr}(X_{N+1:N+M}|X_{1:N})$, from which we compute the posterior distribution of the number of new variants in the follow-up study.

Technically there is a fixed, and finite, upper bound on the number of possible variants established by the (necessarily finite) size of any individual genome. But this bound is usually much larger (often by orders of magnitude) than the number of observed variants. In practice, moreover, we typically expect that no study of any practical finite size N will reveal all possible variants – simply because some variants are so exceedingly rare. *Bayesian nonparametric* methods allow us to avoid hard-coding an unwieldy, large finite bound that may cause computational and modeling headaches. In particular, Bayesian nonparametric methods allow the observed number of variants to be finite for any finite dataset and grow without bound, in such a way that computation typically scales closely with the actual number of variants observed. The mechanism by which Bayesian nonparametric methods work is that we imagine a countable infinity of *latent* variants; thus, for any N , there are always more latent variants to draw on in future. In order to use Bayesian nonparametric methods, then, we provide a label to each of the latent infinity of variants: $\{\psi_j\}_{j=1}^{\infty}$. In particular, we write $X_n := \sum_{j=1}^{\infty} x_{n,j} \delta_{\psi_j}$; since $x_{n,j} = 0$ for all of the unobserved variants, this equation can be considered equivalent to the previous definition of X_n above.

Following all existing methods for estimating new-variant cardinality [Ionita-Laza et al., 2009, Gravel, 2014, Zou et al., 2016, Orlitsky et al., 2016, Chakraborty et al., 2019], we make the modeling assumption that in fact every variant appears independently of every other variant; that is, $x_{n,j}$ is independent of $x_{n,k}$ across all n for $j \neq k$. In reality and by contrast to this assumption, nearby positions on a genome can be highly correlated; this phenomenon is called *linkage disequilibrium*. However, our assumption has two principle advantages: (i) it makes our computations much easier; (ii) it is supported by our state-of-the-art empirical results in Section 6. We also make the milder modeling assumption that our organisms are (infinitely) *exchangeable*.

Roughly, we assume that the order in which we observe the sample organisms is immaterial for any sample size N . Since, for the moment, we assume variant observation is flawless, this assumption presently translates into an exchangeability assumption on the observed data. More precisely, let $[N] := \{1, \dots, N\}$, and let σ_N represent a permutation of $[N]$. Then, for the variant with label ψ_j , for any N and any σ_N , we assume $\text{pr}(x_{1,j}, \dots, x_{N,j}) = \text{pr}(x_{\sigma_N(1),j}, \dots, x_{\sigma_N(N),j})$. Indeed, if we expected systematic variation among organisms in our population between earlier and later samples, we would find it difficult to predict future data from past data without knowing more about the nature of the variation.

Exchangeability of $\{x_{n,j}\}_{n=1}^{\infty}$ implies the existence of a latent, random variant frequency θ_j such that the $x_{n,j}$ are Bernoulli draws with frequency θ_j , independently and identically distributed across n [de Finetti, 1931]. We pair each θ_j together with its associated variant label ψ_j in a measure $\Theta := \sum_{j=1}^{\infty} \theta_j \delta_{\psi_j}$, and we assume the X_n are independent and identical conditional on Θ . We say that X_1 given Θ is described by a *Bernoulli process* (BeP) with parameter Θ , and we write $X_n | \Theta \stackrel{iid}{\sim} \text{BeP}(\Theta)$. The law of the *three-parameter beta process* (3BP) is a convenient and flexible nonparametric prior for the Bernoulli process [Teh and Gorur, 2009, Broderick et al., 2012]. In agreement with our assumption of independence of the $\{x_{n,j}\}_{n=1}^{\infty}$ across j , the three-parameter beta process can be interpreted as a sequence of independent priors on the θ_j . In essence, this process provides control over these independent priors in a way that satisfies our goals: (G1) a finite number of observed variants in any finite sample; (G2) a number of observed variants that is unbounded as the number of samples grows. Furthermore, the three-parameter beta process is able to capture power laws [Teh and Gorur, 2009, Broderick et al., 2012], which are common in physical processes. In particular, its three parameters are: (i) a *mass parameter* α that scales the total number of variants observed; (ii) a *discount parameter* σ that controls the power law of the growth in observed variant cardinality; (iii) a *concentration parameter* c that modulates the frequency of more widespread variants.

We conclude this section by detailing two equivalent representations for drawing $\Theta \sim 3\text{BP}(\alpha, \sigma, c)$. Our focus will be on generating the θ_j . For our purposes here, the ψ_j serve merely to distinguish the variants (with no other significance to the labels), so it is enough to ensure that they are all almost surely distinct. To that end, in what follows, we always take $\psi_j \stackrel{iid}{\sim} \text{Uniform}[0, 1]$, independently and identically distributed across j . For our first representation, we can write $\Theta \sim 3\text{BP}(\alpha, \sigma, c)$ if

$$\Theta = \sum_{i=1}^{\infty} \sum_{j=1}^{C_i} B_{i,j}^{(i)} \prod_{\ell=1}^{i-1} \left(1 - B_{i,j}^{(\ell)}\right) \delta_{\psi_{i,j}},$$

where $C_i \stackrel{iid}{\sim} \text{Poisson}(\alpha)$ and $B_{i,j}^{(\ell)} \stackrel{indep}{\sim} \text{Beta}(1 - c, \sigma + \ell c)$, independently across i , j , and ℓ . This size-biased representation [Broderick et al., 2012, Paisley et al., 2012, Campbell et al., 2019] shows that the 3BP can be interpreted as a sequence of independent frequencies. In mathematical manipulations, though, the Poisson process representation of the beta process is often much more convenient. We therefore note that the representation above is equivalent [Broderick et al., 2012, Paisley et al., 2012]

to drawing the $\{\theta_j\}$ from a Poisson point process with the following rate measure

$$\nu(d\theta) = \alpha \frac{\Gamma(1+c)}{\Gamma(1-\sigma)\Gamma(c+\sigma)} \theta^{-1-\sigma} (1-\theta)^{c+\sigma-1} \mathbf{1}_{[0,1]}(\theta) d\theta. \quad (1)$$

To ensure that aforesaid goals G1 and G2 are satisfied, we must have the following restrictions on the 3BP hyperparameters: $\alpha > 0$, $c > -\sigma$, and $\sigma \in (0, 1)$ [Teh and Gorur, 2009, James, 2017, Broderick et al., 2018]. We discuss in detail the problem of choosing these hyperparameters in practice in Section 6.

3 Predicting the number of new variants

In Section 2 we introduced, and motivated, a Bayesian nonparametric model consisting of: (i) a prior distribution $\Theta \sim 3BP(\alpha, \sigma, c)$ over variant frequencies and (ii) a likelihood function $X_n | \Theta \stackrel{iid}{\sim} \text{BeP}(\Theta)$ for observed variants conditioned on variant frequencies. Under this model, in the present section we predict the number of new variants in a follow-up study after an initial pilot study. Then, we incorporate more realistic assumptions with respect to observation noise, and we derive the first Bayesian nonparametric predictor for new variants that allows experimental conditions to change between studies. Proofs of the results presented in this section are deferred to Appendix A.

3.1 Initial proposals for prediction

We start by deriving the posterior predictive distribution of the number of new variants in a follow-up sample. Then, the expected value of the posterior predictive distribution is a natural Bayesian nonparametric predictor, minimizing risk under square error loss, of the number of new variants in a follow-up sample. With a slight abuse of notation, for any two random variables X and Y defined on the same probability space we denote by $X | Y$ the random variable whose distribution coincides with the conditional distribution of X given Y . We write $\mathcal{N}(\mu, \rho^2)$ for a Gaussian distribution with mean μ and variance ρ^2 . Finally, we write the rising factorial as $(a)_{b\uparrow} = \prod_{i=1}^b (a+b+i-1) = \Gamma(a+b)/\Gamma(a)$.

Proposition 1 (Number of new variants). *Let $\Theta \sim 3BP(\alpha, \sigma, c)$, and let $X_n | \Theta \stackrel{iid}{\sim} \text{BeP}(\Theta)$ for $n = 1, 2, \dots$. Assume $\alpha > 0$, $c > -\sigma$ and $\sigma \in (0, 1)$. Let $U_N^{(M)}$ represent the number of new variants in a follow-up sample of size M after a preliminary study of size N . I.e., we count the variants that do not occur in the preliminary N samples but do occur in the follow-up M samples:*

$$U_N^{(M)} := \sum_{j=1}^{\infty} \mathbf{1} \left(\sum_{n=1}^N x_{n,j} = 0 \right) \mathbf{1} \left(\sum_{m=1}^M x_{N+m,j} > 0 \right). \quad (2)$$

Then

$$U_N^{(M)} | X_{1:N} \sim \text{Poisson} \left\{ \alpha \sum_{m=1}^M \frac{(c+\sigma)_{(N+m-1)\uparrow}}{(c+1)_{(N+m-1)\uparrow}} \right\}. \quad (3)$$

Given Proposition 1, our predictor of the number of new variants in the follow-up is

$$P_N^{(M)} := \mathbb{E} \left(U_N^{(M)} \mid X_{1:N} \right) = \alpha \sum_{m=1}^M \frac{(c + \sigma)_{(N+m-1)\uparrow}}{(c + 1)_{(N+m-1)\uparrow}}.$$

Next we show that $U_N^{(M)} \mid X_{1:N}$ exhibits the desired power-law growth in the number of samples. It also grows *almost surely* according to a particular power law, which is entirely defined by the hyperparameters of the three-parameter beta process. We detail this behavior in the following result, together with a characterization of the asymptotic noise around the posterior predictive mean.

Proposition 2 (Asymptotics for number of new variants). *Under the setting of Proposition 1*

$$\frac{U_N^{(M)}}{M^\sigma} \Big| X_{1:N} \xrightarrow{a.s.} \xi \quad \text{as } M \rightarrow \infty, \quad (4)$$

where $\xi := \frac{\alpha \Gamma(c+1)}{\sigma \Gamma(c+\sigma)}$. The limit (4) holds almost surely with respect to the conditional law of $U_N^{(M)}$ given $X_{1:N}$. Also,

$$\sqrt{M^\sigma} \left(\frac{U_N^{(M)}}{M^\sigma} - \xi \right) \Big| X_{1:N} \xrightarrow{w} \mathcal{N}(0, \xi) \quad \text{as } M \rightarrow \infty. \quad (5)$$

The limit (5) holds weakly (or in distribution) with respect to the conditional law of $U_N^{(M)}$ given $X_{1:N}$.

$P_N^{(M)}$ counts the number of new variants in a follow-up study. Besides that, researchers might be interested in relatively rare new variants, since these are known to play a role in disease predisposition [Cirulli and Goldstein, 2010, Saint Pierre and Génin, 2014, Bomba et al., 2017]. The next result extends Proposition 1 by considering the posterior predictive distribution of the number $U_N^{(M,r)}$ of new variants that will occur r times in the follow-up study. The values of $U_N^{(M,r)}$ for r between 1 and R can be added together to produce the number $U_N^{(M,\leq R)}$ of variants with at most R occurrences in the follow-up. A suitably chosen R then encodes a notion of rareness.

Proposition 3 (Number of new rare variants). *Assume the model in Proposition 1. Let $U_N^{(M,r)}$ represent the number of new variants that occur r times in a follow-up sample of size M after a preliminary study of size N . I.e., we count the variants that do not occur in the preliminary N samples but then occur r times in the follow-up M samples. Let $U_N^{(M,\leq R)}$ similarly represent the number of new variants that occur at most R times. Here $r, R \in [M]$. Define*

$$U_N^{(M,r)} := \sum_{j=1}^{\infty} \mathbf{1} \left(\sum_{n=1}^N x_{n,j} = 0 \right) \mathbf{1} \left(\sum_{m=1}^M x_{N+m,j} = r \right).$$

Then

$$U_N^{(M,r)} \mid X_{1:N} \sim \text{Poisson}(\lambda_r), \quad (6)$$

for $\lambda_r := \alpha \binom{M}{r} \frac{(1-\sigma)_{(r-1)\uparrow} (c+\sigma)_{(N+M-r)\uparrow}}{(c+1)_{(N+M-1)\uparrow}}$. Moreover, for

$$U_N^{(M,\leq R)} := \sum_{r=1}^R U_N^{(M,r)},$$

it holds

$$U_N^{(M,\leq R)} \mid X_{1:N} \sim \text{Poisson} \left(\sum_{r=1}^R \lambda_r \right).$$

Again, the Bayesian nonparametric predictors of $U_N^{(M,r)}$ and $U_N^{(M,\leq R)}$ correspond to the expected values of $U_N^{(M,r)} \mid X_{1:N}$ and $U_N^{(M,\leq R)} \mid X_{1:N}$, respectively, i.e. the parameters of the posterior predictive Poisson distributions displayed in (6). Similarly to Proposition (2), the large M asymptotic behaviour of $U_N^{(M,r)} \mid X_{1:N}$ and $U_N^{(M,\leq R)} \mid X_{1:N}$ display very specific power law behavior almost surely.

Proposition 4 (Asymptotics for number of new rare variants). *Under the setting of Proposition 3,*

$$\frac{U_N^{(M,r)}}{M^\sigma} \Big| X_{1:N} \xrightarrow{a.s.} \xi_r \text{ as } M \rightarrow \infty, \quad (7)$$

and

$$\frac{U_N^{(M,\leq R)}}{M^\sigma} \Big| X_{1:N} \xrightarrow{a.s.} \sum_{r=1}^R \xi_r \text{ as } M \rightarrow \infty, \quad (8)$$

where $\xi_r := \frac{\alpha}{r!} (1-\sigma)_{(r-1)\uparrow} \frac{\Gamma(c+1)}{\Gamma(c+\sigma)}$. The limits hold almost surely with respect to the conditional law of $U_N^{(M,r)}$ given $X_{1:N}$ and the conditional law of $U_N^{(M,\leq R)}$ given $X_{1:N}$, respectively. Also,

$$\sqrt{M^\sigma} \left(\frac{U_N^{(M,r)}}{M^\sigma} - \xi_r \right) \Big| X_{1:N} \xrightarrow{w} \mathcal{N}(0, \xi_r) \text{ as } M \rightarrow \infty \quad (9)$$

and

$$\sqrt{M^\sigma} \left(\frac{U_N^{(M,\leq R)}}{M^\sigma} - \sum_{r=1}^R \xi_r \right) \Big| X_{1:N} \xrightarrow{w} \mathcal{N} \left(0, \sum_{r=1}^R \xi_r \right) \text{ as } M \rightarrow \infty. \quad (10)$$

The limits displayed in Equation (9) and Equation (10) hold weakly (or in distribution) with respect to the conditional law of $U_N^{(M,r)}$ given $X_{1:N}$ and the conditional law of $U_N^{(M,\leq R)}$ given $X_{1:N}$, respectively.

Our analyses reveal some key issues with the Bayesian nonparametric predictors arising from Propositions 1 and 3. First and foremost, they exhibit weak dependence on the observed variants in the preliminary sample of size N . Indeed, notably, the posterior predictive distributions of $U_N^{(M)}$, $U_N^{(M,r)}$ and $U_N^{(M,\leq R)}$ depend on $X_{1:N}$ *only* via the initial sample size N ; see Equation (3) and Equation (6). The actual values of $X_{1:N}$ are immaterial. And we see this behavior borne out in that the asymptotics of these predictors are entirely determined by the hyperparameters of the three-parameter beta process, not by the observed data, even via N ; see Equations (4) and (5) and their counterparts Equations (8) and (9). Thus, without further modification, we would essentially not be using directly any information from our data in our predictors. The crucial modification proposed below in Section 4 will be to *learn* the hyperparameters of the three-parameter beta process in an empirical Bayes procedure from the observed data $X_{1:N}$. Thus, while the work in this section establishes a model or form to fit, the hard work of prediction will be accomplished by the fits of these hyperparameters to the sample $X_{1:N}$.

Next, we observe that the posterior predictive distributions obtained in Propositions 1 and 3, as well as the existing literature on other predictors for the number of new variants in a follow-up study [Ionita-Laza et al., 2009, Gravel, 2014, Zou et al., 2016, Orlitsky et al., 2016, Chakraborty et al., 2019], presume variants are always observed under the same conditions and do not account for how improved variant observation quality may incur a larger cost. But conditions may change between pilot and follow-up experiments, and these changes may be informed by an experimental budget. Therefore, in what follows in Section 3.2, we show how our general Bayesian nonparametric framework can be adapted to the case where variants are not observed perfectly, and in fact we show how we can adapt to different experimental conditions between the pilot and follow-up. We then build on ideas from the work of Ionita-Laza and Laird [2010] to show that we can optimize for the best conditions, to yield the most variants, in the follow-up. That is, in Section 3.2, we consider the challenging problem of optimal allocation of a fixed budget between quality and quantity in genetic experiments: spending resources for sequencing a greater number of genomes (quantity) or spending resources for sequencing genomes with increased accuracy (quality).

3.2 Accounting for sequencing errors

We start by extending the Bayesian nonparametric predictors of Section 3.1 in order to account for non-trivial sequencing error. So far, we have assumed that if any organism exhibits a variant, that variant is detected; i.e., $x_{nj} = 1$ for organism n . However, in practice, sequencing a genome is a complex and noisy process; millions of reads of fragments of the same genomic sequence need to be aligned and compared to the reference genome. Every position j of the genome of individual n is read a random number $D_{n,j}$ of times. That is, $D_{n,j}$ is the (random) sequencing depth of the process. Out of these $D_{n,j}$ times, $D_{n,j,\text{err}}$ reads give rise to an error, due to technological imperfections, and are discarded. Here, $0 \leq D_{n,j,\text{err}} \leq D_{n,j}$. The remaining $D_{n,j,\text{noerr}} = D_{n,j} - D_{n,j,\text{err}}$ reads are correctly processed, aligned to the reference genome, and recorded [Ionita-Laza and Laird, 2010]. Every error-free read can either

agree with the reference genome, or disagree. Let $C_{n,j} \in \{0, 1, \dots, D_{n,j,\text{noerr}}\}$ denote the number of times that reads are correctly processed and we observe disagreement with the reference genome. Finally, a variant is said to be “called” whenever some discrepancy criterion, i.e. the “variant calling rule,” is satisfied.

Following Ionita-Laza and Laird [2010], we focus on simple threshold variant calling rules. That is, a variant is called whenever a sufficient number of reads disagree with the reference genome. Given the threshold value $T > 0$, variation is declared if the count $C_{n,j}$ exceeds T , i.e. $x_{n,j} = \mathbf{1}(C_{n,j} \geq T)$. Furthermore, we make the following assumptions: (i) the sequencing depth $D_{n,j}$ is a Poisson random variable with parameter $\lambda > 0$, which we refer to as the sequencing quality; (ii) the reads are independently and identically distributed across individuals and positions; (iii) the number of successful reads $D_{n,j,\text{noerr}}$ is a Binomial random variable with parameter $(D_{n,j}, 1 - p_{\text{err}})$. The parameter p_{err} is a fixed probability of reading error that depends on the sequencing technology. Under these modeling assumptions, we can write the probability, $\phi(\lambda, T, p_{\text{err}})$, that at least T successful reads are obtained at any position j for any individual n :

$$\phi(\lambda, T, p_{\text{err}}) := \sum_{t=T}^{\infty} \frac{e^{-\lambda} \lambda^t}{t!} \sum_{i=T}^t \binom{t}{i} (1 - p_{\text{err}})^i p_{\text{err}}^{t-i} \quad (11)$$

$$= \sum_{t \geq T} \frac{e^{-\lambda(1-p_{\text{err}})} \{\lambda(1-p_{\text{err}})\}^t}{t!} \leq 1. \quad (12)$$

See Appendix A.6 for a proof of this fact. Note that ϕ is modulated by λ , which controls the sequencing depth and can be set by the practitioner.

Ionita-Laza and Laird [2010] considered the setting in which a single study might happen in the future. In this section, unlike the work of Ionita-Laza and Laird [2010], we assume that we have access to data from a pilot study when designing a follow-up study. When designing the follow-up study under a fixed budget constraint, there is a natural trade-off between the quality of individuals sequenced, measured in terms of the sequencing depth, and the quantity of individuals sequenced. We will discuss in Section 5 how this experimental design question fits in our Bayesian nonparametric framework. In what follows, we will drop the notational dependence on $(\lambda, T, p_{\text{err}})$. Rather we write ϕ and use subscripts to denote potentially different values of ϕ across experiments. For instance, the practitioner may choose a sequencing depth in the follow-up experiment that is different from the sequencing depth in the preliminary experiment. Hence we write ϕ_{pilot} for the pilot experiment and ϕ_{follow} for the follow-up. Our methods can be immediately extended to the case where there are multiple initial experiments with different ϕ values.

After these considerations, we note that our prior distribution over the variant frequencies has not changed: $\Theta \sim 3\text{BP}(\alpha, \sigma, c)$. But now we first draw whether organism n has variant with frequency θ_j according to $\text{Bernoulli}(\theta_j)$. If the organism does have the variant, we draw whether we observe the variant according to $\text{Bernoulli}(\phi_{\text{pilot}})$ in the pilot experiment and $\text{Bernoulli}(\phi_{\text{follow}})$ in the follow-up. Equivalently, we write $X_n \mid \Theta \stackrel{iid}{\sim} \text{BeP}(\phi_{\text{pilot}}\Theta)$ for our pilot experiment likelihood and $X_{N+m} \mid \Theta \stackrel{iid}{\sim} \text{BeP}(\phi_{\text{follow}}\Theta)$ for our follow-up experiment likelihood. The draws are independent

and identically distributed across $n \in [N]$ in the former case and $m \in [M]$ in the latter case. Now we can derive analogous results to Propositions 1 and 3, which had assumed perfect observations.

Proposition 5 (Number of new variants with noisy observation). *Let $\Theta \sim 3BP(\alpha, \sigma, c)$ and $X_n \mid \Theta \sim \text{BeP}(\phi_{\text{pilot}}\Theta)$, independently and identically distributed across $n \in [N]$. Let $X_{n+m} \mid \Theta \sim \text{BeP}(\phi_{\text{follow}}\Theta)$ independently and identically distributed across $m \in [M]$. Assume $\alpha > 0$, $c > -\sigma$ and $\sigma \in (0, 1)$. Then for $U_N^{(M)}$ defined in Equation (2), we have that $U_N^{(M)}$ is almost surely finite with distribution*

$$U_N^{(M)} \mid X_{1:N} \sim \text{Poisson}(\gamma), \quad (13)$$

where

$$\begin{aligned} \gamma &:= \sum_{m=1}^M \int_{\theta=0}^1 \text{Bernoulli}(1 \mid \phi_{\text{follow}}\theta) \text{Bernoulli}(0 \mid \phi_{\text{follow}}\theta)^{m-1} \times \\ &\quad \times \text{Bernoulli}(0 \mid \phi_{\text{pilot}}\theta)^N \nu(d\theta) \\ &= \alpha \phi_{\text{follow}} \sum_{m=1}^M \mathbb{E}_B \{ (1 - \phi_{\text{follow}}B)^{m-1} (1 - \phi_{\text{pilot}}B)^N \}, \end{aligned}$$

for $B \sim \text{Beta}(\theta \mid 1 - \sigma, c + \sigma)$.

Similarly, for $U_N^{(M,r)}$ and $U_N^{(M,\leq R)}$ defined in Proposition 3 with $r, R \in [M]$, we have that these quantities are almost surely finite with respective distributions

$$U_N^{(M,r)} \mid X_{1:N} \sim \text{Poisson}(\gamma_r), \quad U_N^{(M,\leq R)} \mid X_{1:N} \sim \text{Poisson}\left(\sum_{r=1}^R \gamma_r\right), \quad (14)$$

where

$$\begin{aligned} \gamma_r &:= \binom{M}{r} \int_{\theta=0}^1 \text{Bernoulli}(1 \mid \phi_{\text{follow}}\theta)^r \text{Bernoulli}(0 \mid \phi_{\text{follow}}\theta)^{M-r} \\ &\quad \times \text{Bernoulli}(0 \mid \phi_{\text{pilot}}\theta)^N \nu(d\theta) \\ &= \alpha \binom{M}{r} \phi_{\text{follow}}^r \frac{(1+c)_{(r-1)\uparrow}}{(1-\sigma)_{(r-1)\uparrow}} \mathbb{E}_B \{ (1 - \phi_{\text{follow}}B)^{M-r} (1 - \phi_{\text{pilot}}B)^N \}, \end{aligned}$$

for $B \sim \text{Beta}(\theta \mid r - \sigma, c + \sigma)$.

As in the case of perfect sequencing, we wish to derive predictors that we can use in practice – namely, functions only of the observed data. For the same risk-minimization reasons as before, we take the posterior predictive means to be these predictors. We again use the notation $P_N^{(M)}$, $P_N^{(M,r)}$, $P_N^{(M,\leq R)}$, respectively. The previous predictors we defined with this same notation in Section 3.1 can be seen to represent the special case of our updated definitions with $\phi_{\text{pilot}} = \phi_{\text{follow}} = 1$.

4 Empirics for the prediction

Our more realistic model of variant observation sets up a prediction framework for the number of new variants in a follow-up experiment. But without further development, we still face the difficulty that our predictor in Equation (3) does not use any information about the pilot experimental data except its cardinality. Recall that the hyperparameters α, σ, c control the behavior of the predictor, as proved in Section 3. So we will induce a dependency on the observed pilot data by fitting these hyperparameter values to the pilot data. Our approach may be seen to fit into the framework of empirical Bayes.

One common option in empirical Bayes is to maximize the probability of the data given the hyperparameters: $\arg \max_{\alpha, \sigma, c} \text{pr}(X_{1:N} | \alpha, \sigma, c)$ with $\text{pr}(X_{1:N} | \alpha, \sigma, c) = \int_{\Theta} \text{pr}(X_{1:N} | \Theta) \text{pr}(d\Theta | \alpha, \sigma, c)$. In the case without sequencing errors, this probability can be expressed in closed form as the *exchangeable feature probability function* (EFPF) [Broderick et al., 2013]. However, with sequencing errors, the integral can be very high-dimensional and expensive to compute with Markov chain Monte Carlo. Moreover, even without sequencing errors, the exchangeable feature probability function for the beta process is a complex function of sums, products, quotients, and exponentiation of gamma functions [Broderick et al., 2013, Eq. 8], which we find can suffer from numerical instability in this optimization problem.

A much easier choice is to treat the prediction from our model above as a regression function with its own parameters α, σ, c . We can fit these parameters to the pilot project data by imagining subsets of the true pilot data as mini-pilot projects themselves and directly minimizing error in prediction on the remaining data. In particular, consider index $n \in [N]$ as the size of the imagined mini-pilot. Then, by our earlier definition, $P_n^{(m)}$ is the prediction for the number of new variants in the next m data points given the first n data points. Here we write $P_n^{(m)}(\alpha, \sigma, c)$ to emphasize the hyperparameter dependence. Similarly, by our definition in Equation (2), $U_n^{(m)} | X_{1:N}$ is the true number of new variants in the next m data points (for m such that $n + m \leq N$) given the first n data points. Then we solve the error minimization problem:

$$\hat{\alpha}, \hat{\sigma}, \hat{c} := \arg \min_{\substack{\alpha, \sigma, c: \\ \alpha > 0, \sigma \in [0, 1], c > -\sigma}} \sum_{m=1}^{N-n} \left(P_n^{(m)}(\alpha, \sigma, c) - \left(U_n^{(m)} | X_{1:N} \right) \right)^2. \quad (15)$$

In practice, we set $n = \lfloor 2/3 \times N \rfloor$ – a choice that works well across all datasets considered. To find $\hat{\alpha}, \hat{\sigma}, \hat{c}$ via Equation (15), we use the differential evolution algorithm [Storn and Price, 1997], as implemented in SciPy [Jones et al., 2001]. We also considered using multiple folds of the pilot study – in the style of cross validation, instead of a single train-test split. In our experiments, we did not observe a noticeable difference between our proposal in Equation (15) and this more involved procedure. We choose to minimize the 2-norm (sum of squared differences), but Equation (15) can be straightforwardly adapted for other standard choices of error (e.g., 1-norm). Finally, we use the quantity $\hat{P}_N^{(M)} := P_N^{(M)}(\hat{\alpha}, \hat{\sigma}, \hat{c})$ as our predictor for the number of new variants in the follow-up study of size M after observing data from the pilot study of size N .

5 Sequencing errors and optimal experimental design

Now we have finally built up the necessary infrastructure to be able to optimize experimental design decisions about the follow-up study. In particular, our goal is to maximize the number of variants we expect to observe under a fixed budget constraint. To see how the budget comes into play, note that there are two cost sources we have considered for the follow-up study. In particular, it costs more to increase the number of samples M since sequencing each additional sample adds an additional cost. Likewise, it costs more to increase the quality of each sample, where increasing quality is accomplished by increasing the sequencing quality in the followup, λ_{follow} . We might encode the total cost as a function of these two specifications: $f(M, \lambda_{\text{follow}})$. Here, f is increasing in both of its arguments. Conversely, we expect to discover more variants as either of M or λ_{follow} increases and fewer variants as either quantity decreases. Therefore, we face a tradeoff in where to best allocate experimental budget between M and λ_{follow} .

Our framework allows us to precisely quantify and optimize this tradeoff. In particular, we now emphasize the dependence of $\hat{P}_N^{(M)}$ on λ_{follow} , via ϕ_{follow} , by writing $\hat{P}_N^{(M, \lambda_{\text{follow}})}$ for $\hat{P}_N^{(M)}$ computed with λ_{follow} . Since we can compute $\hat{P}_N^{(M, \lambda_{\text{follow}})}$ across values of M and λ_{follow} using Equation (13), we can optimize to find the maximum possible predicted variants under some budget B . And we are typically interested in the experimental settings under which this maximum is achieved:

$$\arg \max_{M, \lambda_{\text{follow}}} \hat{P}_N^{(M, \lambda_{\text{follow}})} \quad \text{subject to} \quad f(M, \lambda_{\text{follow}}) \leq B. \quad (16)$$

To the best of our knowledge, no previous methods – including [Ionita-Laza et al., 2009, Ionita-Laza and Laird, 2010, Gravel, 2014, Zou et al., 2016, Orlitsky et al., 2016, Chakraborty et al., 2019] – have been designed or modified to predict variants under different experimental conditions in a follow-up study given results from a pilot. Relatedly, no methods, prior to our own, exist to solve the optimal experimental design problem in Equation (16). We believe the Bayesian hierarchical modeling framework we adopt here allows a particularly straightforward way to incorporate the potential for different sequencing depths, and more generally different experimental setups, in different phases of the study. Notably, Ionita-Laza and Laird [2010] consider experimental design – but only for a single future study, without observing any (pilot) data. Given its Bayesian grounding, their associated predictor might be adapted to our pilot and follow-up framework using similar techniques to those we introduce above. But we will see in Section 6 that the quality of their predictor is much worse than that of our method; any corresponding experimental design would therefore suffer. We suspect our gains are due to the flexibility of the Bayesian nonparametric framework and ability to capture power laws in the data.

Note that practitioners might instead be interested in maximizing the number of new rare variants in the follow-up study (i.e., variants that appear at most R times in the follow-up sample). In this case, we again take the empirical Bayes estimates of hyperparameters $\hat{\alpha}, \hat{\sigma}, \hat{c}$ found via Equation (15). Analogous to the notation for $\hat{P}_N^{(M, \lambda_{\text{follow}})}$, we let $\hat{P}_N^{(M, \leq R, \lambda_{\text{follow}})}$ represent our predictor $P_N^{(M, \leq R)}$ (for the number of

new rare variants) with hyperparameter values set to $\hat{\alpha}, \hat{\sigma}, \hat{c}$ and follow-up sequencing quality set to λ_{follow} . Then, to maximize the number of new rare variants, the following optimization problem would be more appropriate than Equation (16):

$$\arg \max_{M, \lambda_{\text{follow}}} \hat{P}_N^{(M, \leq R, \lambda_{\text{follow}})} \quad \text{subject to} \quad f(M, \lambda_{\text{follow}}) \leq B. \quad (17)$$

We highlight that we still suggest learning the hyperparameters $\hat{\alpha}, \hat{\sigma}, \hat{c}$ via the original optimization problem – importantly, using the full predictor of all new variants. We make this recommendation since rare variants may be sparser in the pilot study and thereby provide less information about these hyperparameters. The optimization problem in Equation (17) then uses our best guess for the behavior of the underlying variant frequencies to optimize the number of new rare variants $\hat{P}_N^{(M, \leq R, \lambda_{\text{follow}})}$.

6 Experiments

6.1 Experimental setup

We evaluate our methods on both synthetic and real data. Our real-data experiments use the Genome Aggregation Database (gnomAD) [Karczewski et al., 2019], a recent extension of the Exome Aggregation Consortium (ExAC) data set [Lek et al., 2016] and the largest publicly available human genomic dataset. GnomAD contains genetic information from 125,748 individual exome sequences recorded at 1,195,872 genomic loci. Samples in gnomAD are arranged into eight subpopulations according to geographic origin, where one of the eight subpopulations is a catch-all category called “Other”. These subpopulations vary in size from 1,335 Bulgarian samples to 17,720 African-American samples. Following Zou et al. [2016], we treat each subpopulation as a distinct dataset. Our figures in the main text focus on the Bulgarian, Korean, Ashkenazi-Jewish, and “Other” subgroups since these are the smallest and thus most challenging. Results on the remaining populations can be found in Appendix F.

6.2 Prediction with no sequencing errors

A number of existing methods predict the number of new variants in a follow-up study under the assumption of perfect recovery of variants. These approaches use, respectively parametric Bayesian methods [Ionita-Laza et al., 2009], linear programming [Gravel, 2014, Zou et al., 2016], a harmonic jackknife [Gravel, 2014], and a smoothed version of the classic Good-Toulmin estimator [Chakraborty et al., 2019]. We encountered numerical issues with the linear programming method of Gravel [2014] and so, like Zou et al. [2016], we do not include it in our comparison. Even in their original paper, Gravel [2014] did not report superior performance of their linear programming approach over their other method, the harmonic jackknife [Gravel, 2014], which we do include in our comparison. To assess prediction error in each case, we use an approach akin to cross validation. Namely, we treat each subpopulation as a dataset. We divide the subpopulation into 33 folds of equal size. For a smaller number of folds, each fold represents a larger pilot study. All methods improve when the pilot study is

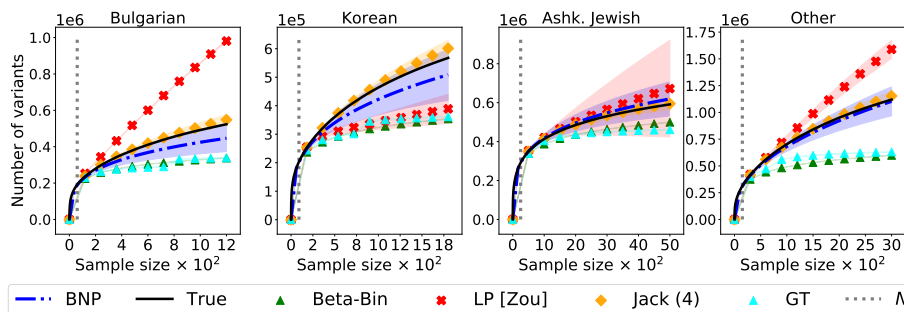


Figure 1: Predicting the number of new variants in a follow-up study under constant experimental conditions. The solid black line displays the true number of distinct variants (vertical axis) as the sample size increases (horizontal axis). Lines for each method are averaged across all folds; see Section 6.2 (blue: our method, Bayesian nonparametric (BNP), Eq. (3); green: Ionita-Laza et al. [2009]; red: Zou et al. [2016]; orange: Gravel [2014] (4th order), cyan: Chakraborty et al. [2019]). Shaded regions show one standard deviation across folds.

increased substantially in size, i.e. when there is more information in the pilot. We find that the choice of 33 folds creates a challenging scenario with a small amount of pilot information. Nonetheless, both our method and the harmonic jackknife still perform well in these conditions. We consider each fold in turn as data from the pilot study and treat the remaining data (i.e., the data not in this fold) as the follow-up. We follow [Zou et al., 2016] to make a visual summary of our results; namely, we plot the mean number of variants across all folds as a function of data set size in the pilot, and we plot the mean number of total predicted variants (across both pilot and follow-up) as a function of data set size in the same plot. A vertical dashed line marks the pilot size. Shaded regions indicate one empirical standard deviation, measured across the folds. We include the exact values in the plot for comparison. Figure 1 demonstrates that our method matches the exact value more closely than the parametric Bayesian approach [Ionita-Laza et al., 2009], the linear programming approach [Zou et al., 2016] and the nonparametric smoothed Good-Toulmin method [Chakraborty et al., 2019]. And our method has roughly the same performance in the case of perfect observation as the jackknife approach [Gravel, 2014].

In Appendix F we run both the Bayesian parametric approach and our method on data simulated under the parametric Bayesian model used by Ionita-Laza et al. [2009]. We also run both methods on data simulated under the 3-parameter beta process model we propose above; see Appendix F.2. We find that the approach of Ionita-Laza et al. [2009] provides excellent predictions when the data is generated under their assumed model – but deteriorates in performance under the simulated 3-parameter beta process data, as for real data. Therefore, we believe the parametric Bayesian method suffers on real data due to the assumed Ionita-Laza et al. [2009] model being ill adapted for real-life power laws.

Zou et al. [2016] use a linear program to estimate *rare* variant frequencies; they

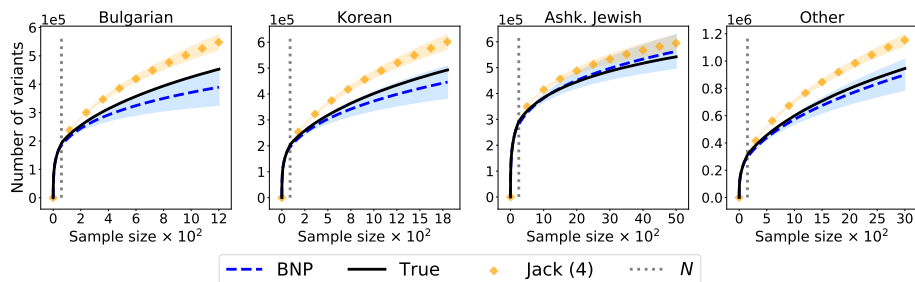


Figure 2: Predicting the number of new variants under different experimental conditions between the pilot and follow-up. Same four subpopulations (gnomAD). Pilot sequencing quality is $\lambda_{\text{pilot}} = 45$. Follow-up sequencing quality is $\lambda_{\text{follow}} = 32$. Horizontal axis is the number of samples. Vertical axis is the number of total observed variants across both pilot and follow-up. The threshold $T = 30$.

approximate frequencies of common variants with the empirical frequency. “Rare” is defined to be any frequency less than $\kappa/100$, for some user-defined threshold $\kappa \in (0, 100)$, interpreted as a percent. In practice, we found that the output of the algorithm is very sensitive to the choice of κ (see Appendix F.4). The authors suggest $\kappa = 1$ as a default setting, but we observed numerical instability and poor predictive performance for this choice. This observation holds especially when the pilot size N is small, which we believe to be a particular case of interest in designing experiments for further data collection (i.e., for the follow-up study). For instance, we expect the small- N case to arise frequently in the study of non-model organisms [Russell et al., 2017]. In Figure 1, we chose $\kappa = 20$, which led to convergence of the optimization algorithm in all cases. We explore other values of κ in Appendix F.4.

6.3 Prediction under different experimental conditions

We now turn to the case where there may be sequencing errors in the pilot, in the follow-up, or both. And the sequencing quality may differ between the pilot and the follow-up. No existing method works in this case. Since, like our method, the method of Ionita-Laza et al. [2009] is Bayesian, we believe it could be straightforwardly adapted using similar ideas to the ones we present here. But we have already seen that our Bayesian nonparametric method provides much more accurate predictions in the case of no sequencing errors, so we believe it is more fruitful to develop the Bayesian nonparametric approach. Similarly, we believe the linear programming approach [Zou et al., 2016] might be adapted to the special case where the follow-up is more error prone than the pilot. But even this development would still leave open the case where the follow-up might be made more accurate by increasing sequencing quality – and we have already observed that the Bayesian nonparametric approach provides better, more automatic predictions in the case of error-free observation. Finally, while the jackknife approach performs very well in the case with no sequencing errors, we do not think it will be as straightforward to adapt to the case where sequencing quality

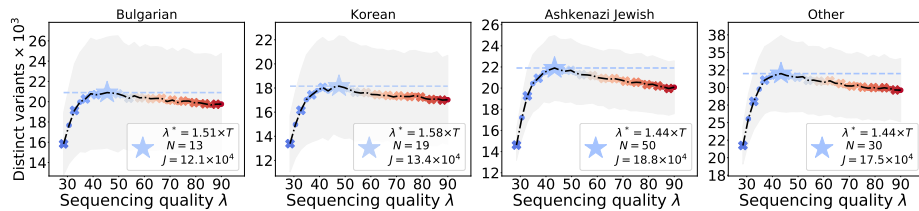


Figure 3: Designing an experiment to maximize the number of new variants in a follow-up study. Same four subpopulations (gnomAD). Horizontal axis is the follow-up sequencing quality λ_{follow} . Vertical axis is the predicted number of observed variants in the follow-up by maximizing M under the budget B and quality λ_{follow} .

may change between the pilot and follow-up.

In Figure 2 we see that there is indeed a noticeable difference in the number of observed variants when the experimental conditions change between the pilot and follow-up. In particular, we consider a pilot sequencing quality $\lambda_{\text{pilot}} = 45$ and a follow-up sequencing quality $\lambda_{\text{follow}} = 32$. We use a fixed threshold $T = 30$, a standard coverage value in human genomic experiments [Karczewski et al., 2019]. To represent this change between studies, we use the gnomAD data as in Section 6.2 but apply additional thinning to simulate imperfect observation due to sequencing depth (see Appendix F.1 for additional details). Since the jackknife is not able to use information about the changing sequencing depth, we expect our Bayesian nonparametric method to deliver superior predictive performance when sequencing quality changes. This behavior is exactly what we see in Figure 2.

6.4 Designing experiments to maximize the number of observed variants

Finally, we demonstrate that our Bayesian nonparametric predictor can be used for experimental design in practice. Our procedure consists of three steps. (1) Given the pilot data and sequencing quality λ_{pilot} , we minimize Equation (15) to estimate the parameters c, σ, α . (2) Next, we consider a range of values of the follow-up sequencing quality λ_{follow} . For each λ_{follow} , we choose the maximum follow-up size M that stays within our budget B . And we use the learned values of the parameters c, σ, α to predict the number of new variants in each case. (3) We choose the settings of λ_{follow} and M that maximize the number of new variants. We illustrate this procedure in Figure 3.

In our experiments, we set the cost function $f(M, \lambda_{\text{follow}}) = M \log(\lambda_{\text{follow}})$ as in Ionita-Laza and Laird [2010], budget $D = 3000$, threshold $T = 30$, error $p_{\text{err}} = 0.01$ and $\lambda_{\text{pilot}} = 40$. We run the procedure over all folds, plot the empirical mean line, and plot the shaded region to illustrate one standard deviation. We see a tradeoff in quality and quantity in Figure 3. Namely, maximizing quantity M leads to very small values of λ_{follow} to maintain the budget B . With sufficiently low quality, though, fewer variants are discovered. Conversely, when λ_{follow} is set very high, we require a very small M to maintain the budget B , and not many variants are discovered. Intermediate values of λ_{follow} and M serve to maximize the number of variants discovered under a

fixed budget.

7 Discussion

We have presented a Bayesian nonparametric method for predicting the number of variants in a follow-up study using information from a preliminary study. Our method works even when the follow-up study has different experimental conditions from the preliminary study and can be used for optimal design of the follow-up study. Here we have focused on the case where genetic sequences can be represented as a collection of binary observations – variants and not-variants. But our method can be extended in a straightforward manner to encode and predict different types of variants. In particular, we here use a beta process to generate variant frequencies, and a Bernoulli process conditional on these frequencies to generate their presence in individual genomes. But, using the Bayesian nonparametric conjugacy framework of James [2017], Broderick et al. [2018], we could instead use a categorical (or *multinoulli*) likelihood process with a conjugate Bayesian nonparametric prior for the now-multiple frequencies per variant location. In the present work, we have also focused on the case where we have a single study of preliminary data: the pilot. But our same modeling framework can be used to accommodate multiple different pilot studies. To this aim, we would – just as in our main development – generate the variant frequencies according to a beta process. And in turn generate the observed variants in each study with different damped Bernoulli processes. The ultimate effect would be to introduce more distinct, but workable, Bernoulli terms in Equation (13). Finally, we have provided code for our experiments at https://bitbucket.org/masoero/moreforless_bayesiandiscovery/src/master.

Acknowledgments

The authors thank Joshua Schraiber and Brian Trippe for useful discussions. Federico Camerlenghi and Stefano Favaro received funding from the European Research Council (ERC) under the European Union’s Horizon 2020 research and innovation programme under grant agreement No 817257. Federico Camerlenghi and Stefano Favaro gratefully acknowledge the financial support from the Italian Ministry of Education, University and Research (MIUR), “Dipartimenti di Eccellenza” grant 2018–2022. Lorenzo Masoero and Tamara Broderick were supported in part by DARPA, the CSAIL-MSR Trustworthy AI Initiative, an NSF CAREER Award, a Sloan Research Fellowship, and ONR.

References

- P. Berti, I. Crimaldi, L. Pratelli, and P. Rigo. Central limit theorems for an Indian buffet model with random weights. *The Annals of Applied Probability*, 25(2):523–547, 2015.

- L. Bomba, K. Walter, and N. Soranzo. The impact of rare and low-frequency genetic variants in common disease. *Genome biology*, 18(1):77, 2017.
- T. Broderick, M. I. Jordan, and J. Pitman. Beta processes, stick-breaking and power laws. *Bayesian Analysis*, 7(2):439–476, 2012.
- T. Broderick, J. Pitman, and M. I. Jordan. Feature allocations, probability functions, and paintboxes. *Bayesian Analysis*, 8(4):801–836, 2013.
- T. Broderick, A. C. Wilson, and M. I. Jordan. Posteriors, conjugacy, and exponential families for completely random measures. *Bernoulli*, 24(4B):3181–3221, 2018.
- K. P. Burnham and W. S. Overton. Estimation of the size of a closed population when capture probabilities vary among animals. *Biometrika*, 65(3):625–633, 1978.
- T. Campbell, D. Cai, and T. Broderick. Exchangeable trait allocations. *Electronic Journal of Statistics*, 12(2):2290–2322, 2018.
- T. Campbell, J. H. Huggins, J. P. How, and T. Broderick. Truncated random measures. *Bernoulli*, 25(2):1256–1288, 2019.
- S. Chakraborty, A. Arora, C. B. Begg, and R. Shen. Using somatic variant richness to mine signals from rare variants in the cancer genome. *Nature Communications*, 10: 5506, 2019.
- E. T. Cirulli and D. B. Goldstein. Uncovering the roles of rare variants in common disease through whole-genome sequencing. *Nature Reviews Genetics*, 11(6):415, 2010.
- A. Clauset, C. R. Shalizi, and M. E. Newman. Power-law distributions in empirical data. *SIAM review*, 51(4):661–703, 2009.
- . G. P. Consortium. A global reference for human genetic variation. *Nature*, 526(7571): 68, 2015.
- B. de Finetti. Funzione caratteristica di un fenomeno aleatorio. *Atti della R. Accademia Nazionale dei Lincei, Ser. 6. Memorie, Classe di Scienze Fisiche, Matematiche e Naturali 4*, pages 251–299, 1931.
- B. Efron and R. Thisted. Estimating the number of unseen species: How many words did Shakespeare know? *Biometrika*, 63(3):435–447, 1976.
- R. A. Fisher, A. S. Corbet, and C. B. Williams. The relation between the number of species and the number of individuals in a random sample of an animal population. *The Journal of Animal Ecology*, pages 42–58, 1943.
- I. Good and G. Toulmin. The number of new species, and the increase in population coverage, when a sample is increased. *Biometrika*, 43(1-2):45–63, 1956.
- S. Gravel. Predicting discovery rates of genomic features. *Genetics*, 197(2):601–610, 2014.

- S. Gravel, B. M. Henn, R. N. Gutenkunst, A. R. Indap, G. T. Marth, A. G. Clark, F. Yu, R. A. Gibbs, C. D. Bustamante, and D. L. Altshuler. Demographic history and rare allele sharing among human populations. *Proceedings of the National Academy of Sciences*, 108(29):11983–11988, 2011.
- N. L. Hjort. Nonparametric Bayes estimators based on beta processes in models for life history data. *The Annals of Statistics*, 18(3):1259–1294, 1990.
- I. Ionita-Laza and N. M. Laird. On the optimal design of genetic variant discovery studies. *Statistical Applications in Genetics and Molecular Biology*, 9(1), 2010.
- I. Ionita-Laza, C. Lange, and N. M. Laird. Estimating the number of unseen variants in the human genome. *Proceedings of the National Academy of Sciences*, 106(13):5008–5013, 2009.
- L. F. James. Bayesian Poisson calculus for latent feature modeling via generalized Indian Buffet Process priors. *The Annals of Statistics*, 45(5):2016–2045, 2017.
- E. Jones, T. Oliphant, and P. Peterson. SciPy: open source scientific tools for Python, 2001. URL <http://www.scipy.org>.
- K. J. Karczewski, L. C. Francioli, G. Tiao, B. B. Cummings, J. Alföldi, Q. Wang, R. L. Collins, K. M. Laricchia, A. Ganna, and D. P. Birnbaum. Variation across 141,456 human exomes and genomes reveals the spectrum of loss-of-function intolerance across human protein-coding genes. *BioRxiv*, page 531210, 2019.
- Y. Kim. Nonparametric Bayesian estimators for counting processes. *Annals of Statistics*, pages 562–588, 1999.
- M. Lek, K. J. Karczewski, E. V. Minikel, K. E. Samocha, E. Banks, T. Fennell, A. H. O’Donnell-Luria, J. S. Ware, A. J. Hill, and B. B. Cummings. Analysis of protein-coding genetic variation in 60,706 humans. *Nature*, 536(7616):285, 2016.
- A. Lijoi, R. H. Mena, and I. Prünster. Bayesian nonparametric estimation of the probability of discovering new species. *Biometrika*, 94(4):769–786, 2007.
- I. Mathieson and D. Reich. Differences in the rare variant spectrum among human populations. *PLoS genetics*, 13(2):e1006581, 2017.
- A. Orlitsky, A. T. Suresh, and Y. Wu. Optimal prediction of the number of unseen species. *Proceedings of the National Academy of Sciences*, 113(47):13283–13288, 2016.
- J. Paisley, D. Blei, and M. Jordan. Stick-breaking beta processes and the poisson process. In *Artificial Intelligence and Statistics*, pages 850–858, 2012.
- J. A. Reuter, D. V. Spacek, and M. P. Snyder. High-throughput sequencing technologies. *Molecular cell*, 58(4):586–597, 2015.

- J. J. Russell, J. A. Theriot, P. Sood, W. F. Marshall, L. F. Landweber, L. Fritz-Laylin, J. K. Polka, S. Oliferenko, T. Gerbich, A. Gladfelter, et al. Non-model model organisms. *BMC biology*, 15(1):55, 2017.
- A. Saint Pierre and E. Génin. How important are rare variants in common disease? *Briefings in functional genomics*, 13(5):353–361, 2014.
- A. N. Shiryaev. *Probability (2Nd Ed.)*. Springer-Verlag, Berlin, Heidelberg, 1995. ISBN 0-387-94549-0.
- G. Sirugo, S. M. Williams, and S. A. Tishkoff. The missing diversity in human genetic studies. *Cell*, 177(1):26–31, 2019.
- R. Storn and K. Price. Differential evolution—a simple and efficient heuristic for global optimization over continuous spaces. *Journal of global optimization*, 11(4):341–359, 1997.
- C. F. Taylor and G. R. Taylor. Current and emerging techniques for diagnostic mutation detection. In *Molecular Diagnosis of Genetic Diseases*, pages 9–44. Springer, 2004.
- Y. W. Teh and D. Gorur. Indian buffet processes with power-law behavior. In *Advances in Neural Information Processing Systems*, pages 1838–1846, 2009.
- R. Thibaux and M. I. Jordan. Hierarchical Beta processes and the Indian buffet process. In *Artificial Intelligence and Statistics*, pages 564–571, 2007.
- F. G. Tricomi and A. Erdélyi. The asymptotic expansion of a ratio of gamma functions. *Pacific Journal of Mathematics*, 1(1):133–142, 1951.
- J. Zou, G. Valiant, P. Valiant, K. Karczewski, S. O. Chan, K. Samocha, M. Lek, S. Sunyaev, M. Daly, and D. G. MacArthur. Quantifying unobserved protein-coding variants in human populations provides a roadmap for large-scale sequencing projects. *Nature Communications*, 7:13293, 2016.
- O. Zuk, S. F. Schaffner, K. Samocha, R. Do, E. Hechter, S. Kathiresan, M. J. Daly, B. M. Neale, S. R. Sunyaev, and E. S. Lander. Searching for missing heritability: designing rare variant association studies. *Proceedings of the National Academy of Sciences*, 111(4):E455–E464, 2014.

A Additional results and proofs

A.1 Proof of Proposition 1

Proof. By construction, the variant frequencies $\{\theta_j\}$ are formed from a Poisson point process with rate measure ν given in Equation (1). Recall that a variant with frequency θ_j appears in organism n with Bernoulli probability θ_j , independently across n . Therefore, the collection of variant frequencies whose corresponding variants have not yet appeared after N organisms comes from a thinned Poisson point process relative to the original Poisson point process generating the $\{\theta_j\}$; the thinned process has rate measure $\nu(d\theta) \cdot \text{Bernoulli}(0|\theta)^N$ and is independent of the collection of frequencies that did appear in the first N organisms. Similarly, the collection of variant frequencies corresponding to variants that did not appear in the first N organisms but then did appear in the first follow-up organism comes from a thinned Poisson point process with rate measure $\nu(d\theta) \cdot \text{Bernoulli}(0|\theta)^N \cdot \text{Bernoulli}(1|\theta)$ and is independent of the collection of frequencies that did not appear in the first $N+1$ organisms. Recursively, for $m \geq 1$, the collection of variant frequencies corresponding to variants that did not appear in the first $N+m-1$ organisms but then did appear in the m th follow-up organism comes from a thinned Poisson point process with rate measure

$$\begin{aligned}
& \nu(d\theta) \text{Bernoulli}(0|\theta)^{N+m-1} \text{Bernoulli}(1|\theta) \\
&= \alpha \frac{\Gamma(1+c)}{\Gamma(1-\sigma)\Gamma(c+\sigma)} \theta^{-1-\sigma+1} (1-\theta)^{c+\sigma-1+N+m-1} \mathbf{1}_{[0,1]}(\theta) d\theta \\
&= \alpha \frac{\Gamma(1+c)}{\Gamma(1-\sigma)\Gamma(c+\sigma)} \cdot \frac{\Gamma(1-\sigma)\Gamma(c+\sigma-1+N+m)}{\Gamma(c+N+m)} \\
&\quad \cdot \text{Beta}(\theta | 1-\sigma, c+\sigma-1+N+m) d\theta \\
&= \alpha \frac{(c+\sigma)_{(N+m-1)\uparrow}}{(1+c)_{(N+m-1)\uparrow}} \text{Beta}(\theta | 1-\sigma, c+\sigma-1+N+m) d\theta.
\end{aligned}$$

Finally, we observe that the number of points in a Poisson point process is Poisson distributed with mean equal to the integral of its rate measure. Each of these Poisson point processes is independent, and the sum of independent Poissons is Poisson with mean equal to the sum of the means. So, since $U_N^{(M)}$ is the sum of points in these M Poisson point processes with $m \in [M]$, we have $U_N^{(M)}$ is Poisson with mean

$$\begin{aligned}
& \sum_{m=1}^M \int_0^1 \alpha \frac{(c+\sigma)_{(N+m-1)\uparrow}}{(1+c)_{(N+m-1)\uparrow}} \text{Beta}(\theta | 1-\sigma, c+\sigma-1+N+m) d\theta \\
&= \sum_{m=1}^M \alpha \frac{(c+\sigma)_{(N+m-1)\uparrow}}{(1+c)_{(N+m-1)\uparrow}},
\end{aligned}$$

as was to be shown. □

A.2 Proof of Proposition 2

In the following we make use of the O notation, indeed we will write $f(x) = O(g(x))$ to mean that the ratio $|f(x)/g(x)|$ is a bounded function of the variable x . A preliminary result is needed.

Lemma 6. *For any $c > 0$, $N \geq 1$ and $\sigma \in (0, 1)$ we have that*

$$\frac{1}{M^\sigma} \sum_{m=1}^M \frac{\Gamma(c + N + m - 1 + \sigma)}{\Gamma(c + N + m)} = \frac{1}{\sigma} + O(M^{-\sigma}) \quad (18)$$

is satisfied as M grows to $+\infty$.

Proof. As in the proof of Berti et al. [2015, Lemma 2], we know that for any $x > 0$,

$$\frac{\Gamma(x + \sigma)}{\Gamma(x + 1)} = x^{\sigma-1}(1 + g(x)),$$

where $g : (0, +\infty) \rightarrow \mathbb{R}$ is such that $\sup_{x \geq 0} |g(x)x| < +\infty$. Putting $x = c + N + m - 1$, where $m \geq 1$ while c and N are fixed constants, this very last condition on g is equivalent to $\sup_{y \geq c+N-1} |g(y)y| < +\infty$. Hence there exists $K > 0$ such that $|g(y)| \leq K/y$ for any $y \geq c + N - 1$. With this in mind we focus on the left hand side of Equation (18) in the statement of Lemma 6:

$$\frac{1}{M^\sigma} \sum_{m=1}^M \frac{\Gamma(c + N + m - 1 + \sigma)}{\Gamma(c + N + m)} \quad (19)$$

$$= \frac{1}{M^\sigma} \sum_{m=1}^M (c + N + m - 1)^{\sigma-1} (1 + g(c + N + m - 1))$$

$$= \frac{1}{M^\sigma} \sum_{m=1}^M (c + N + m - 1)^{\sigma-1} \quad (20)$$

$$+ \frac{1}{M^\sigma} \sum_{m=1}^M (c + N + m - 1)^{\sigma-1} g(c + N + m - 1). \quad (21)$$

As for the sum of Equation (20) note that the following inequalities hold true

$$\begin{aligned} \frac{(c + N + M)^\sigma - (c + N)^\sigma}{\sigma M^\sigma} &= \int_1^{M+1} \frac{(c + N + m - 1)^{\sigma-1}}{M^\sigma} dm \\ &\leq \sum_{m=1}^M \frac{(c + N + m - 1)^{\sigma-1}}{M^\sigma} \\ &\leq \int_0^M \frac{(c + N + m - 1)^{\sigma-1}}{M^\sigma} dm \\ &= \frac{(c + N + M - 1)^\sigma - (c + N - 1)^\sigma}{\sigma M^\sigma}, \end{aligned} \quad (22)$$

where we have used the fact that $(c + N + m - 1)^{\sigma-1}$ is decreasing in m , and used the corresponding integrals to bound the sum. We can use an asymptotic expansion of the upper and the lower bound in Equation (22) to get

$$\begin{aligned} \frac{1}{\sigma} \left(\frac{\sigma(c+N)}{M} + o\left(\frac{1}{M}\right) - \frac{(c+N)^\sigma}{M^\sigma} \right) &\leq \sum_{m=1}^M \frac{(c+N+m-1)^{\sigma-1}}{M^\sigma} - \frac{1}{\sigma} \\ &\leq \frac{1}{\sigma} \left(\frac{\sigma(c+N-1)}{M} + o\left(\frac{1}{M}\right) - \frac{(c+N-1)^\sigma}{M^\sigma} \right), \end{aligned}$$

which entails that

$$\sum_{m=1}^M \frac{(c+N+m-1)^{\sigma-1}}{M^\sigma} = \frac{1}{\sigma} + O\left(\frac{1}{M^\sigma}\right). \quad (23)$$

As for Equation (21), we exploit the properties of g to get

$$\begin{aligned} &\left| \frac{1}{M^\sigma} \sum_{m=1}^M (c+N+m-1)^{\sigma-1} g(c+N+m-1) \right| \\ &\leq \frac{K}{M^\sigma} \sum_{m=1}^M (c+N+m-1)^{\sigma-2} \\ &\leq \frac{K}{M^\sigma} \int_{c+N-1}^{c+N+M-1} \frac{1}{x^{2-\sigma}} dx \\ &= \frac{K}{M^\sigma(1-\sigma)} \times \left(\frac{1}{(c+N-1)^{1-\sigma}} - \frac{1}{(c+N+M-1)^{1-\sigma}} \right) \end{aligned}$$

The last inequality implies that

$$\frac{1}{M^\sigma} \sum_{m=1}^M (c+N+m-1)^{\sigma-1} g(c+N+m-1) = \frac{1}{M^\sigma} O\left(\frac{1}{M}\right). \quad (24)$$

Putting Equation (22) and Equation (24) in Equation (20) and Equation (21) the thesis follows. \square

If X is a real valued random element, we denote by $\Phi_X(t) = E(e^{itX})$ its characteristic function, where i is the imaginary unit.

Proof of Proposition 2. We start by showing the strong law of large numbers of Equation (4) in the main text. We denote by P_N the probability P given $X_{1:N}$ and by E_N and Var_N the expected valued and the variance given $X_{1:N}$. From Lemma 6 we deduce that

$$\frac{E_N(U_N^{(M)})}{M^\sigma} = \frac{\alpha}{M^\sigma} \frac{\Gamma(c+1)}{\Gamma(c+\sigma)} \sum_{m=1}^M \frac{\Gamma(c+\sigma+N+m-1)}{\Gamma(c+N+m)} \rightarrow \frac{\alpha\Gamma(c+1)}{\sigma\Gamma(c+\sigma)} \quad (25)$$

as $M \rightarrow +\infty$. We observe that $U_N^{(M)} = H_N^{(1)} + \dots + H_N^{(M)}$, where $H_N^{(m)}$ are independent Poisson random variables with mean

$$\frac{\alpha(c + \sigma)_{N+m-1\uparrow}}{(c + 1)_{N+m-1\uparrow}},$$

for $m = 1, \dots, M$ and M is arbitrary large. $H_N^{(m)}$ is the number of new variants that have been observed in the $N+m$ -th individual, conditionally on the first N individuals. As a consequence we may write

$$\frac{U_N^{(M)} - E_N(U_N^{(M)})}{M^\sigma} = \frac{H_N^{(1)} - E_N(H_N^{(1)}) + \dots + H_N^{(M)} - E_N(H_N^{(M)})}{M^\sigma}.$$

The Kronecker's lemma [Shiryayev, 1995, Lemma IV.3.2] implies that

$$\lim_{M \rightarrow +\infty} \frac{U_N^{(M)} - E_N(U_N^{(M)})}{M^\sigma} = 0 \quad P_N - \text{almost surely,}$$

provided that the following condition is satisfied

$$\sum_{m=1}^{+\infty} \frac{\text{Var}_N(H_N^{(m)})}{m^{2\sigma}} < +\infty. \quad (26)$$

This may be easily verified as follows:

$$\begin{aligned} \sum_{m=1}^{+\infty} \frac{\text{Var}_N(H_N^{(m)})}{m^{2\sigma}} &= \sum_{m=1}^{+\infty} \frac{\alpha}{m^{2\sigma}} \frac{(c + \sigma)_{N+m-1\uparrow}}{(c + 1)_{N+m-1\uparrow}} \\ &= \alpha \frac{\Gamma(c + 1)}{\Gamma(c + \sigma)} \sum_{m=1}^{+\infty} \left\{ \frac{1}{m^{2\sigma}} \frac{\Gamma(c + \sigma + N + m - 1)}{\Gamma(c + N + m)} \right\} < +\infty. \end{aligned}$$

The series turns out to be convergent because the following asymptotic relation holds true:

$$\frac{\Gamma(c + \sigma + N + m - 1)}{\Gamma(c + N + m)} \sim \frac{\alpha}{m^{1+\sigma}} \frac{\Gamma(c + 1)}{\Gamma(c + \sigma)}.$$

Hence Equation (26) is satisfied, so we conclude that

$$\lim_{M \rightarrow +\infty} \frac{U_N^{(M)} - E_N(U_N^{(M)})}{M^\sigma} = 0 \quad \text{almost surely,}$$

which is equivalent to the thesis thanks to Equation (25).

We now prove the central limit theorem stated in Equation (5) in the main text. We prove the result using the convergence of characteristic functions. We use the fact that the posterior distribution of $U_N^{(M)}$ is Poisson to evaluate the characteristic function a

posteriori: for convenience, let $\tilde{U}_N^{(M)} := \sqrt{M^\sigma} \left(\frac{U_N^{(M)}}{M^\sigma} - \xi \right)$, where we recall that ξ is defined as

$$\xi := \frac{\alpha \Gamma(c+1)}{\sigma \Gamma(c+\sigma)}.$$

Then,

$$\begin{aligned} \Phi_{\tilde{U}_N^{(M)} | X_{1:N}}(t) &= E_N \left[\exp \left\{ it \tilde{U}_N^{(M)} \right\} \right] \\ &= \exp \left\{ -it\xi\sqrt{M^\sigma} + \alpha(e^{it/\sqrt{M^\sigma}} - 1) \sum_{m=1}^M \frac{(c+\sigma)_{N+m-1\uparrow}}{(c+1)_{N+m-1\uparrow}} \right\} \\ &= \exp \left\{ -it\xi\sqrt{M^\sigma} + (e^{it/\sqrt{M^\sigma}} - 1) \frac{\alpha\Gamma(c+1)}{\Gamma(c+\sigma)} \sum_{m=1}^M \frac{\Gamma(c+N+m-1+\sigma)}{\Gamma(c+N+m)} \right\}. \end{aligned}$$

We now use Lemma 6 and the asymptotic expansion of the exponential function to get

$$\begin{aligned} \Phi_{\tilde{U}_N^{(M)} | X_{1:N}}(t) &= \\ &= \exp \left\{ -it\xi\sqrt{M^\sigma} + \frac{\alpha\Gamma(c+1)}{\Gamma(c+\sigma)} \left(\frac{it}{\sqrt{M^\sigma}} - \frac{t^2}{2M^\sigma} + O(M^{-\frac{3}{2}\sigma}) \right) \left(\frac{M^\sigma}{\sigma} + O(1) \right) \right\} \\ &= \exp \left\{ -it\xi\sqrt{M^\sigma} + \frac{\alpha}{\sigma} \frac{\Gamma(c+1)}{\Gamma(c+\sigma)} \left(it\sqrt{M^\sigma} - \frac{t^2}{2} + O(\sqrt{M^\sigma}) \right) \right\} \\ &= \exp \left\{ -it\xi\sqrt{M^\sigma} + \xi \left(it\sqrt{M^\sigma} - \frac{t^2}{2} + O(\sqrt{M^\sigma}) \right) \right\} \\ &= \exp \left\{ -\frac{\xi t^2}{2} + O(\sqrt{M^\sigma}) \right\}, \end{aligned}$$

where in the penultimate line we substituted

$$\xi = \frac{\alpha \Gamma(c+1)}{\sigma \Gamma(c+\sigma)}.$$

Therefore, as M grows to infinity, we get

$$\Phi_{\sqrt{M^\sigma} \left(\frac{U_N^{(M)}}{M^\sigma} - \xi \right) | X_{1:N}}(t) \longrightarrow \exp \left\{ -\frac{\xi t^2}{2} \right\},$$

and the thesis follows. \square

A.3 Proof of Proposition 3

Proof. Analogous to the proof of Proposition 1, we consider the Poisson point process $\{\theta_j\}$ and thin it to those frequencies corresponding to variants chosen no times in the

preliminary N samples and chosen exactly r times out of the follow-up M samples. The probability of being chosen to be thinned, then, is $\text{Bernoulli}(0 \mid \theta)^N \cdot \binom{M}{r} \cdot \text{Bernoulli}(0 \mid \theta)^{M-r} \cdot \text{Bernoulli}(1 \mid \theta)^r$. The thinned process therefore has rate measure

$$\begin{aligned}
& \nu(d\theta) \cdot \text{Bernoulli}(0 \mid \theta)^N \cdot \binom{M}{r} \cdot \text{Bernoulli}(0 \mid \theta)^{M-r} \cdot \text{Bernoulli}(1 \mid \theta)^r \\
&= \alpha \frac{\Gamma(1+c)}{\Gamma(1-\sigma)\Gamma(c+\sigma)} \theta^{-1-\sigma+r} (1-\theta)^{c+\sigma-1+N+M-r} d\theta \\
&= \alpha \frac{\Gamma(1+c)}{\Gamma(1-\sigma)\Gamma(c+\sigma)} \frac{\Gamma(r-\sigma)\Gamma(c+\sigma+N+M-r)}{\Gamma(c+N+M)} \times \\
&\quad \times \text{Beta}(r-\sigma, c+\sigma+N+M-r) d\theta \\
&= \alpha \frac{(1-\sigma)_{(r-1)\uparrow} (c+\sigma)_{(N+M-r)\uparrow}}{(1+c)_{(N+M-1)\uparrow}} \text{Beta}(r-\sigma, c+\sigma+N+M-r) d\theta.
\end{aligned}$$

Since $U_N^{(M,r)}$ counts the thinned atoms, it has Poisson distribution with mean equal to the integral of the rate measure, i.e. mean equal to

$$\alpha \frac{(1-\sigma)_{(r-1)\uparrow} (c+\sigma)_{(N+M-r)\uparrow}}{(1+c)_{(N+M-1)\uparrow}}, \quad (27)$$

as was to be shown.

The distribution of $U_N^{(M,\leq R)}$ follows immediately from the observation that the $U_N^{(M,r)}$ are independent Poisson random variables, where the independence is inherited from the independent thinned Poisson point processes. \square

A.4 Proof of Proposition 4

Proof. We start by proving Equation (8) in the main text, but in order to do this we have to define some other statistics:

$$U_N^{(M,\leq R)} := \sum_{r=1}^R U_N^{(M,r)} \quad \text{and} \quad U_N^{(M,\geq R)} := \sum_{r=R}^M U_N^{(M,r)} \quad (28)$$

which have to be respectively interpreted as the number of new genomic variants observed at most R times and the number of new genomic variants observed at least R times. Our strategy is the following: we prove that $U_N^{(M,\geq R)}/M^\sigma$ converges almost surely to a constant and then we use the relation

$$U_N^{(M,R)} = U_N^{(M,\geq R)} - U_N^{(M,\geq R+1)} \quad (29)$$

to prove the convergence of $U_N^{(M,R)}$.

We evaluate the first moment of $U_N^{(M,\geq R)}/M^\sigma$ a posteriori: for notation purpose, let

$\tilde{U}_N^{(M)}$

$$\begin{aligned} \frac{1}{M^\sigma} E_N \left(U_N^{(M, \geq R)} \right) &= \frac{E_n[U_N^{(M)}]}{M^\sigma} - \sum_{r=1}^{R-1} \frac{E_N \left(U_N^{(M, r)} \right)}{M^\sigma} \\ &\rightarrow \frac{\alpha \Gamma(c+1)}{\sigma \Gamma(c+\sigma)} - \alpha \frac{\Gamma(c+1)}{\Gamma(c+\sigma)} \sum_{r=1}^{R-1} \frac{(1-\sigma)_{R-1 \uparrow}}{R!}, \end{aligned} \quad (30)$$

as $M \rightarrow \infty$, where we have used Equation (34) and Equation (25). It then follows that

$$E_N[U_N^{(M, r)}] \asymp c_1 M^\sigma$$

for some positive constant $c_1 > 0$. Besides for the variance of $U_N^{(M, \geq R)}$ we get

$$\begin{aligned} \text{Var}_N \left(U_N^{(M, \geq R)} \right) &= \text{Var}_N \left(U_N^{(M)} - U_N^{(M, \leq R-1)} \right) \\ &= E_N \left\{ U_N^{(M)} - \sum_{r=1}^{R-1} \left(U_N^{(M, r)} \right) - E_N \left(U_N^{(M)} \right) + \sum_{r=1}^{R-1} E_N \left(U_N^{(M, r)} \right) \right\}^2 \\ &\leq E_N \left\{ \left| U_N^{(M)} - E_N \left(U_N^{(M)} \right) \right| + \sum_{r=1}^{R-1} \left| U_N^{(M, r)} - E_N \left(U_N^{(M, r)} \right) \right| \right\}^2 \\ &\leq R \times E_N \left(\left| U_N^{(M)} - E_N \left(U_N^{(M)} \right) \right|^2 + \sum_{r=1}^{R-1} \left| U_N^{(M, r)} - E_N \left(U_N^{(M, r)} \right) \right|^2 \right) \end{aligned}$$

where the last inequality follows by a simple application of the discrete version of the Hölder's inequality. Then, using also the fact that we get that $U_N^{(M)}$ and $U_N^{(M)}$ are Poisson random variable a posteriori, we obtain:

$$\begin{aligned} \text{Var}_N \left(U_N^{(M, \geq R)} \right) &\leq r \left(\text{Var}_N \left(U_N^{(M)} \right) + \sum_{r=1}^{R-1} \text{Var}_N \left(U_N^{(M, r)} \right) \right) \\ &= R \left\{ E_N \left[U_N^{(M)} \right] + \sum_{r=1}^{R-1} E_N \left(U_N^{(M, r)} \right) \right\} \asymp c_2 M^\sigma \end{aligned}$$

where $c_2 > 0$ is a positive constant. From all the previous considerations and by an application of the Markov inequality we obtain that for any $\varepsilon > 0$

$$\begin{aligned} \text{Pr}_N \left\{ \left| \frac{U_N^{(M, \geq R)}}{E_n \left(U_N^{(M, \geq R)} \right)} - 1 \right| \geq \varepsilon \right\} &\leq \frac{\text{Var}_N \left(U_N^{(M, \geq R)} \right)}{\varepsilon^2 \left\{ E_N \left(U_N^{(M, \geq R)} \right) \right\}^2} \\ &\lesssim \frac{c_2 M^\sigma}{\varepsilon^2 (c_1 M^\sigma)^2} \asymp \frac{1}{M^\sigma} \end{aligned} \quad (31)$$

hence we can conclude that the ratio

$$\frac{U_N^{(M, \geq R)}}{E_N \left(U_N^{(M, \geq R)} \right)}$$

converges in probability to 1. Besides if we choose the subsequence $M_k := k^{2/\sigma}$, as $k = 1, 2, \dots$, an application of the first Borel-Cantelli lemma leads us to state that the ratio converges to 1 almost surely. Since $U_N^{(M, \geq R)}$ is an increasing process as M increases, for any M in the interval $\{\lfloor m_k \rfloor, \dots, \lfloor m_{k+1} \rfloor\}$ we have that

$$U_N^{(\lfloor m_k \rfloor, \geq R)} \leq U_N^{(M, \geq R)} \leq U_N^{(\lfloor m_{k+1} \rfloor, \geq R)}$$

where $\lfloor x \rfloor$ denotes the integer part of x . Hence we also have that

$$\frac{U_N^{(\lfloor m_k \rfloor, \geq R)}}{E_N \left(U_N^{(\lfloor m_{k+1} \rfloor, \geq R)} \right)} \leq \frac{U_N^{(M, \geq R)}}{E_N \left(U_N^{(M, \geq R)} \right)} \leq \frac{U_N^{(\lfloor m_{k+1} \rfloor, \geq R)}}{E_N \left(U_N^{(\lfloor m_k \rfloor, \geq R)} \right)}.$$

Leveraging the fact that the lower and upper bound of the central term converge to 1 as $k \rightarrow \infty$,

$$\frac{U_N^{(M, \geq R)}}{E_N [U_N^{(M, \geq R)}]} \rightarrow 1,$$

in an almost sure sense as $M \rightarrow +\infty$. In other words – using Equation (30) – we have just proved that

$$\frac{U_N^{(M, \geq R)}}{M^\sigma} \rightarrow \frac{\alpha \Gamma(c+1)}{\sigma \Gamma(c+\sigma)} - \alpha \frac{\Gamma(c+1)}{\Gamma(c+\sigma)} \sum_{r=1}^{R-1} \left(\frac{(1-\sigma)_{r-1 \uparrow}}{r!} \right), \quad (32)$$

P_N -almost-surely as $M \rightarrow \infty$.

The thesis now follows by Equation (32) and the Equation (29), indeed:

$$\frac{U_N^{(M, R)}}{M^\sigma} = \frac{U_N^{(M, \geq R)}}{M^\sigma} - \frac{U_N^{(M, \leq R+1)}}{M^\sigma} \rightarrow \alpha \frac{\Gamma(c+1)}{\Gamma(c+\sigma)} \frac{(1-\sigma)_{r-1 \uparrow}}{r!},$$

P_N -almost surely as M grows.

To prove Equation (9) in the main text, one has to prove that the characteristic functions converge, more precisely

$$\Phi_{\sqrt{M^\sigma} \left(\frac{U_N^{(M, R)}}{M^\sigma} - \xi_R \right) \Big|_{X_{1:N}}}(t) \rightarrow \exp \left(-\frac{t^2 \xi_R}{2} \right) \quad \text{for any } t \in R,$$

as M goes to infinity.

First of all observe that the (posterior) expectation of $U_N^{(M, R)}$ is such that

$$\begin{aligned} E_N \left(U_N^{(M, R)} \right) &= \alpha \binom{M}{R} \frac{(1-\sigma)_{R-1 \uparrow} (c+\sigma)_{N+M-R}}{(c+1)_{N+M-1 \uparrow}} \\ &= \left(\frac{\Gamma(M+1)}{\Gamma(M-R+1)} \frac{\Gamma(c+\sigma+N+M-R)}{\Gamma(c+N+M)} \right) \times \end{aligned} \quad (33)$$

$$\begin{aligned} &\times \alpha \frac{(1-\sigma)_{R-1 \uparrow} \Gamma(c+1)}{\Gamma(R+1) \Gamma(c+\sigma)} \\ &= M^\sigma (1 + o(M^{-1})) \alpha \frac{(1-\sigma)_{R-1 \uparrow} \Gamma(c+1)}{\Gamma(R+1) \Gamma(c+\sigma)}, \end{aligned} \quad (34)$$

where we have used the asymptotic expansion of ratios of gamma functions given by Tricomi and Erdélyi [1951]. Let $\tilde{U}_N^{(M,R)} := \sqrt{M^\sigma} \left(\frac{U_N^{(M,R)}}{M^\sigma} - \xi_R \right)$. Using the expansion given in Equation (34) it is easy to see that

$$\begin{aligned} \Phi_{\tilde{U}_N^{(M,R)} \mid X_{1:N}}(t) &= \\ &= \exp \left\{ -it\sqrt{M^\sigma}\xi_R + M^\sigma\xi_R(1 + o(M^{-1})) \left(\frac{it}{\sqrt{M^\sigma}} + \frac{t^2}{2M^\sigma} + o(M^{-1+\sigma}) \right) \right\} \\ &= \exp \left\{ -\frac{t^2\xi_R}{2} + o(1) \right\}, \end{aligned}$$

therefore the thesis follows. \square

A.5 Proof of Proposition 5

Proof. To see the almost sure finiteness of the Poisson parameter and hence of the random variables $U_N^{(M)}$ and of $U_N^{(M,r)}$, and $U_N^{(M,\leq R)}$, note that the parameter constraints for the three-parameter beta process are specifically constructed so that $\theta\nu(d\theta)$ is a proper beta distribution; see the end of section 2 and James [2017], Broderick et al. [2018]. The θ factor will arise from $\text{Bernoulli}(1 \mid \phi_{\text{follow}}\theta)$.

The exact form of the Poisson parameter in Equation (13) arises by following the same thinning argument as in the proof of Proposition 1. To see the beta representation,

$$\begin{aligned} &\text{Bernoulli}(1 \mid \phi_{\text{follow}}\theta)\text{Bernoulli}(0 \mid \phi_{\text{follow}})^{m-1}\text{Bernoulli}(0 \mid \phi_{\text{pilot}})^N \nu(d\theta) \\ &= \alpha \frac{\Gamma(1+c)}{\Gamma(1-\sigma)\Gamma(c+\sigma)} \theta^{-1-\sigma} ((1-\theta)^{c+\sigma-1}) \times \\ &\times (\phi_{\text{follow}}\theta)(1-\phi_{\text{follow}}\theta)^{m-1} (1-\phi_{\text{pilot}}\theta)^N \mathbf{1}_{[0,1]}(\theta) d\theta \\ &= \alpha \frac{\Gamma(1+c)}{\Gamma(1-\sigma)\Gamma(c+\sigma)} \phi_{\text{follow}} (1-\phi_{\text{follow}}\theta)^{m-1} (1-\phi_{\text{pilot}}\theta)^N \cdot \frac{\Gamma(1-\sigma)\Gamma(c+\sigma)}{\Gamma(c+1)} \\ &\cdot \text{Beta}(\theta \mid 1-\sigma, c+\sigma) d\theta \\ &= \alpha \phi_{\text{follow}} \text{Beta}(\theta \mid 1-\sigma, c+\sigma) d\theta. \end{aligned}$$

The exact form of the Poisson parameter γ_r in Equation (14) arises by following the

same thinning argument as in the proof of Proposition 3. To see the beta representation,

$$\begin{aligned}
& \text{Bernoulli}(1 \mid \phi_{\text{follow}}\theta)^r \text{Bernoulli}(0 \mid \phi_{\text{follow}}\theta)^{M-r} \text{Bernoulli}(0 \mid \phi_{\text{pilot}}\theta)^N \nu(d\theta) \\
&= \alpha \frac{\Gamma(1+c)}{\Gamma(1-\sigma)\Gamma(c+\sigma)} \theta^{-1-\sigma} (1-\theta)^{c+\sigma-1} \times \\
&\quad \times (\phi_{\text{follow}}\theta)^r (1-\phi_{\text{follow}}\theta)^{M-r} (1-\phi_{\text{pilot}}\theta)^N \mathbf{1}_{[0,1]}(\theta) d\theta \\
&= \alpha \frac{\Gamma(1+c)}{\Gamma(1-\sigma)\Gamma(c+\sigma)} \phi_{\text{follow}}^r (1-\phi_{\text{follow}}\theta)^{M-r} (1-\phi_{\text{pilot}}\theta)^N \cdot \frac{\Gamma(r-\sigma)\Gamma(c+\sigma)}{\Gamma(c+r)} \\
&\quad \cdot \text{Beta}(\theta \mid r-\sigma, c+\sigma) d\theta \\
&= \alpha \phi_{\text{follow}}^r \frac{(1+c)_{(r-1)\uparrow}}{(1-\sigma)_{(r-1)\uparrow}} \cdot \text{Beta}(\theta \mid r-\sigma, c+\sigma) d\theta.
\end{aligned}$$

□

A.6 Proof of equivalence of Equation (11) and Equation (12)

We first prove a more general proposition about binomial thinning for Poisson random variables.

Proposition 7 (Binomial thinning of Poisson random variables). *Let $X \sim \text{Poisson}(\lambda)$ and let Y be the random variable obtained by binomially thinning X , i.e. such that $Y \mid X = x \sim \text{Binomial}(x, \tau)$. Then, Y and $X - Y$ are independent random variables with $Y \sim \text{Poisson}(\lambda\tau)$ and $X - Y \sim \text{Poisson}(\lambda(1-\tau))$.*

Proof. To prove this fact, it suffices to show that

$$\Pr(Y = m, X - Y = n) = \text{Poisson}(\tau\lambda; m) \text{Poisson}((1-\tau)\lambda; n)$$

Recall that the conditional distribution of Y given $X = m + n$ is binomial with parameters $m + n$ and τ . Therefore, we can write the joint distribution of $(Y, X - Y)$ as

$$\begin{aligned}
\Pr(Y = m, X - Y = n) &= \Pr(X = m + n) \Pr(Y = m \mid X = m + n) \\
&= \left(\frac{e^{-\lambda} \lambda^{m+n}}{(m+n)!} \binom{m+n}{m} \tau^m (1-\tau)^n \right) \\
&= \left(\frac{(\tau\lambda)^m}{m!} \right) e^{-\tau\lambda} \left(\frac{\{(1-\tau)\lambda\}^n}{n!} \right) e^{-(1-\tau)\lambda}.
\end{aligned}$$

The thesis follows. □

In light of this proposition, it is clear that Equation (11) and Equation (12) are equivalent.

B Bayesian prediction with the Beta-Bernoulli product model

We here review the approach proposed by Ionita-Laza et al. [2009]. The authors consider the same problem of genomic variation described in Section 2.

Ionita-Laza et al. [2009] assume that there exists a finite, albeit unknown, number of loci at which genomic variation can be observed. We denote such quantity with the letter K . Given a pilot study $X = X_{1:N}$ with J distinct variants, we can obtain the site-frequency-spectrum (or fingerprint) of the sample,

$$\mathbf{f}_N = [f_{N,1} \dots, f_{N,J}] \quad \text{with} \quad f_{N,j} = \sum_{\ell=1}^J \mathbf{1} \left(\sum_{n=1}^N x_{n,\ell} = j \right), \quad (35)$$

so that $f_{N,1}$ counts the number of variants observed only once among the N samples, $f_{N,2}$ the number of variants observed in exactly two samples etc. The input data $X_{1:N}$ is here viewed as a binary matrix, $X_{1:N} \in \{0, 1\}^{N \times J}$, in which all positions at which variation is not observed are discarded, and the order of the columns is immaterial. This binary matrix is modeled via a parametric beta-Bernoulli model: the authors assume that there exists a fixed, unknown number $K < \infty$ of loci at which variation can be observed. For each $j \in [K]$, they assume that there exists an associated variant, labelled by index j , displayed by any observation (row) with probability $\theta_j \in [0, 1]$. The frequencies $\theta_j, j = 1, \dots, K$ are distributed according to a beta distribution with parameters a, b , i.e.

$$\boldsymbol{\theta} = [\theta_1 \quad \dots \quad \theta_K], \quad \text{with} \quad \theta_j \sim \text{Beta}(a, b) \quad \forall j,$$

independently and identically distributed. Conditionally on $\boldsymbol{\theta}$,

$$X_n = [x_{n,1} \quad \dots \quad x_{n,K}], \quad \text{with} \quad x_{n,j} \sim \text{Bernoulli}(\theta_j).$$

Therefore, the columns of the matrix $X_{1:N}$ are independently and identically distributed, while the rows are made of independent, but not identically distributed entries. Under this model, the number of counts of each variant is binomially distributed, conditionally on the latent frequency of such variant, i.e.

$$z_{N,j} \mid \theta_j := \sum_{i=1}^n x_{i,j} \mid \theta_j \sim \text{Binomial}(N, \theta_j).$$

Recalling that $f_{N,j} = \sum_{\ell=1}^J \mathbf{1}(z_{N,\ell} = j)$ is the number of variants which appear exactly j times among the first N samples, and letting $g(x; a, b)$ be the density function of a beta random variable with parameters a, b evaluated at x ,

$$g(x; a, b) = \frac{x^{a-1}(1-x)^{b-1}}{\mathbf{B}(a, b)} \mathbf{1}_{[0,1]}(x),$$

with $B(a, b) = \int_0^1 x^{a-1}(1-x)^{b-1} dx = \Gamma(a)\Gamma(b)/\Gamma(a+b)$, then the probability that exactly j of the N individuals show variation at a given site is given by

$$\begin{aligned} p_{N,j} &= \int_0^1 \binom{N}{j} \theta^j (1-\theta)^{N-j} g(\theta; a, b) d\theta \\ &= \binom{N}{j} \int_0^1 \frac{\theta^{N+a-1} (1-\theta)^{N-j+b-1}}{\mathbf{B}(a, b)} d\theta = \binom{N}{j} \frac{(a)_{j\uparrow} (b)_{N-j\uparrow}}{(a+b)_{N\uparrow}}. \end{aligned} \quad (36)$$

Because we can't observe more than N variants in N trials, and since we don't know anything about variants which are yet to be observed, probabilities of Equation (36) are then normalized as follows:

$$\lambda_{N,j} = \frac{p_{N,j}}{\sum_{\ell=1}^N p_{N,\ell}} = \frac{\binom{N}{j} (a)_{j\uparrow} (b)_{N-j\uparrow}}{\sum_{\ell=1}^N \binom{N}{\ell} (a)_{\ell\uparrow} (b)_{N-\ell\uparrow}},$$

for all $\ell = 1, \dots, N$. It follows that the log likelihood for the observed data $X_{1:N}$ is given by

$$\ell_{a,b}^{\text{BBPM}}(X_{1:N}) = \log \left(\prod_{j=1}^N \lambda_{N,j}^{f_{N,j}} \right) = \sum_{j=1}^N f_{N,j} \log(\lambda_{N,j}).$$

Notice that the expected number of variants appearing exactly once in a sample of N observations can be computed in closed form,

$$\begin{aligned} \eta_{N,1} &:= \mathbb{E}[f_{N,1}] = \mathbb{E} \left\{ \sum_{j=1}^K \binom{N}{1} \mathbf{1} \left(\sum_{n=1}^N x_{n,j} = 1 \right) \right\} \\ &= KN \int_{[0,1]} \frac{\theta^{a-1} (1-\theta)^{b-1}}{\mathbf{B}(a, b)} \theta (1-\theta)^{N-1} d\theta \\ &= KN \frac{\mathbf{B}(a+1, N+b-1)}{\mathbf{B}(a, b)} = \frac{aKN}{N+b-1} \frac{\mathbf{B}(a, N+b)}{\mathbf{B}(a, b)}, \end{aligned}$$

where we used independence of the variants, linearity of the expectation operator and the properties of the beta function. Letting $M = tN$ be the number of additional samples to be observed, we can compute the expected number of hitherto unseen variants, to be observed in additional M samples after N samples have been collected as

$$\begin{aligned}
\Delta_N(M) &= \mathbb{E} \left[\sum_{j=1}^K \mathbf{1} \left(\sum_{m=1}^M x_{m,j} > 0 \right) \mathbf{1} \left(\sum_{n=1}^N x_{n,j} = 0 \right) \right] \\
&= \frac{K}{\mathbf{B}(a,b)} \int_{[0,1]} (1 - (1-\theta)^{(t+1)N}) - (1 - (1-\theta)^N) \theta^{a-1} (1-\theta)^{b-1} d\theta \\
&= \frac{K}{\mathbf{B}(a,b)} \int_{[0,1]} \left\{ (1-\theta)^N - (1-\theta)^{(t+1)N} \right\} \theta^{a-1} (1-\theta)^{b-1} d\theta \\
&= K \frac{\mathbf{B}(a, N+b)}{\mathbf{B}(a,b)} - K \frac{\mathbf{B}(a, N(t+1)+b)}{\mathbf{B}(a,b)}
\end{aligned}$$

Now, noticing that

$$K \frac{\mathbf{B}(a, N+b)}{\mathbf{B}(a,b)} = \frac{\eta_{N,1}}{a} \frac{N+b-1}{N}$$

and

$$K \frac{\mathbf{B}(a, N(t+1)+b)}{\mathbf{B}(a,b)} = \frac{\eta_{N,1}}{a} \frac{N+b-1}{N} \frac{\mathbf{B}(a, N(t+1)+b)}{\mathbf{B}(a, N+b)},$$

it follows that

$$\Delta_N(M) = \frac{\eta_{N,1}}{a} \frac{N+b-1}{N} \left[1 - \frac{\mathbf{B}(a, N(t+1)+b)}{\mathbf{B}(a, N+b)} \right]. \quad (37)$$

Importantly, $\Delta_N(M)$ depends on K only via $\eta_{N,1}$. To use the estimator $\Delta_N(M)$, Ionita-Laza et al. [2009] substitute $\eta_{N,1}$ with its empirical counterpart $f_{N,1}$, the number of variants which have been observed exactly once in the sample $X_{1:N}$. The parameters a, b are found via maximization of the log-likelihood of the model,

$$\{a^*, b^*\} = \arg \max_{a>0, b>0} \{ \ell_{a,b}^{\text{BBPM}}(X_{1:N}) \}$$

Remark 8. *The estimator obtained in Equation (37) crucially relies on the empirical frequency of variants observed once among the first N draws, $f_{N,1}$. For example, if a dataset had $f_{N,1} = 0$, $\Delta_N(M) = 0$ for every $M > 0$.*

C Linear program to estimate the frequencies of frequencies

Zou et al. [2016] assume, in the same way as Ionita-Laza et al. [2009], that there exists a finite albeit unknown number of sites at which variants can be observed. They formalize the problem of hitherto unseen variants prediction as that of recovering the distribution of frequencies of all the genetic variants in the population, including those variants which have not yet been observed.

They assume that each possible variant in a sample is independent of the other variants, and that the j -th variant appears with a given probability θ_j conditionally independently and identically distributed across all the individuals observed - i.e. the θ_j are parameters of independent Bernoulli random variables $x_{n,j}$ for all $n \geq 1$ and j . Therefore the pilot study $X_{1:N}$ is modeled by a collection of independent Bernoulli random variables, which are also identically distributed along each column, and the sum $z_{N,j} \mid \theta_j := \sum_{n=1}^N x_{n,j} \mid \theta_j \sim \text{Binomial}(N, \theta_j)$. From the frequencies $z_{N,1}, \dots, z_{N,J}$ of the J variants observed among the first N samples, it is possible to compute the fingerprint of the sample, \mathbf{f}_N . Given the fingerprint, the goal is to recover the population's histogram, which is a map quantifying, for every $\theta \in [0, 1]$, the number of variants such that $\theta_j = \theta$. Formally, learn a map h from the distribution of frequencies to integers

$$h : (0, 1] \rightarrow \mathbb{N} \cup \{0\} \quad (38)$$

Because for N large enough the empirical frequencies associated to common variants should be well approximated by their empirical counterpart, Zou et al. [2016] only consider the problem of estimating the histogram from the truncated fingerprint $\mathbf{f}_N^{(\kappa)} = \{f_{N,j} : j/N \leq 100 \times \kappa\}$. In their analysis, the authors only consider $\kappa = 1$, i.e. they consider “common” variants all those variants that appear in more than 1% of the sample elements. Moreover, rather than learning a continuous function as described by Equation (38), they solve a discretized version of the problem. They fix a discretization factor $\delta \geq 1$, and then set up a linear program in which the goal is to correctly estimate the population histogram associated to the frequencies in the set $\mathcal{S} = \{\frac{1}{1000N}, \delta \frac{1}{1000N}, \dots, \delta^i \frac{1}{1000N}, \dots, \kappa\}$. The value δ , given κ , determines how many frequencies are going to be estimated in $(0, \kappa]$: the lower δ , the finer the discretization. The authors suggest using $\delta = 1.05$. In our experiments, we set $\delta = 1.01$, for which we find the method to produce better results, at the cost of a small additional computational effort. Finally, the problem of recovering the histogram is solved through the following optimization:

$$\min_{h(\theta), \theta \in \mathcal{S}} \sum_{j: j \leq N\kappa} \frac{1}{1 + f_{N,j}} \left| f_{N,j} - \sum_{\theta \in \mathcal{S}} h(\theta) \text{Binomial}(N, \theta, j) \right|$$

subject to

$$h(\theta) \geq 0, \sum_{\theta \in \mathcal{S}} h(\theta) \leq K, \sum_{\theta \in \mathcal{S}} \theta \cdot h(\theta) + \sum_{j: j > N\kappa}^J \frac{j}{N} f_{N,j} = \frac{J}{N},$$

where K is an upper bound on the total number of variants, and $\text{Binomial}(N, \theta, j)$ is the probability that a Binomial draw with bias θ and N rounds is equal to j .

Given the histogram \hat{h} which solves the linear program above, one can obtain an estimate of the number of unique variants at any sample size M using

$$V(\hat{h}, M) = \sum_{\theta: \hat{h}(\theta) > 0} \hat{h}(\theta) (1 - (1 - \theta)^M).$$

Following Zou et al. [2016], we refer to this estimator as the “unseenEST” estimator.

D Jackknife estimators

Jackknife estimators for predicting the number of hitherto unseen species were first introduced by in the capture-recapture literature by Burnham and Overton [1978].

Given $X_{1:N} \stackrel{iid}{\sim} F(\psi)$ for some distribution F and some parameter ψ , let $\hat{\psi}_N = \hat{\psi}_N(X_{1:N})$ be an estimator of ψ with the property that

$$\mathbb{E}[\hat{\psi}_N] = \psi + \frac{a_1}{N} + \frac{a_2}{N^2} + \dots, \quad (39)$$

for fixed constants a_1, a_2, \dots . Without loss of generality assume $\hat{\psi}_N$ to be symmetric in its inputs $X_{1:N}$, and denote with $\mathcal{I} \subset [N]$ a subset of given size p , let $\hat{\psi}_{N-p, \mathcal{I}}$ be the estimate obtained by dropping the observations whose indices are in \mathcal{I} . Similarly, let

$$\hat{\psi}_N^{(p)} = \binom{N}{p}^{-1} \sum_{\mathcal{I}: |\mathcal{I}|=p} \hat{\psi}_{N-p, \mathcal{I}} \quad (40)$$

The idea of the Jackknife estimator is that, if the assumption of Equation (39) holds, we can improve over $\hat{\psi}_N$ by using a correction originating from Equation (40). The p -th order Jackknife estimator is defined as

$$\hat{\psi}_N^{J_p} = \frac{1}{p} \sum_{\ell=0}^p \left((-1)^\ell \binom{p}{\ell} (N-\ell)^p \hat{\psi}_N^{(\ell)} \right). \quad (41)$$

Under the assumption of Equation (39), the estimator of Equation (41) has bias approaching zero polynomially fast in the correction order, $\text{Bias}(\hat{\psi}_N^{J_p}) \sim N^{-p-1}$.

D.1 An estimator for the population size

Burnham and Overton [1978] introduced a nonparametric procedure to estimate the total number of animals present in a closed population when capture-recapture data is available. Assume that there is a fixed, but unknown number K of total species. Over the course of N repeated observational experiments, $J \leq K$ distinct species are observed.

Let $X_{1:N}$ be the collection of available data, in which $X_n = [x_{n,1}, \dots, x_{n,J}]$, with $x_{n,j} = 1$ if species j has been observed on the n -th experiment, and 0 otherwise. Moreover, assume that each species $j \in [K]$ – both observed and unobserved ones – is observed across all trials with a fixed, but unknown probability $\theta_j \in (0, 1]$.

Notice that while Burnham and Overton [1978] developed the estimator having in mind a fixed and finite population of animals, we can also think of each sample X_n as a genomic sequence characterized by the presence or absence of genetic variants at different sites.

The nonparametric MLE for the total support size K is given by $\hat{K}_N^{\text{MLE}}(X_{1:N}) = \hat{K}_N^{\text{MLE}} = J$. Clearly $J \leq K$, therefore J is a biased estimate for K . If one assumes, in a similar spirit to Equation (39), that

$$\mathbb{E}[\hat{K}_N^{\text{MLE}}] = K + \frac{a_1}{N} + \frac{a_2}{N^2} + \dots, \quad (42)$$

then one could use the jackknife estimator of Equation (41) to estimate K . This requires computing $\hat{\psi}_N^{(\ell)}$ for $\ell = 1, \dots, p$, which are linear functions of the observed fingerprint f_N .

The case $p = 1$: We outline the approach for $p = 1$. Let $q_{N,n}$ be the number of animals which have been observed only once out of the N trials, exactly on the n -th,

$$q_{N,n} = \sum_{j \geq 1} \mathbf{1}(x_{n,j} = 1) \mathbf{1} \left(\sum_{n' \neq n} x_{n',j} = 0 \right)$$

Then, because $q_{N,1} + \dots + q_{N,N} = f_{N,1}$ by construction,

$$\hat{K}_N^{(1, \setminus n)} = J - q_{N,n} \quad \text{and} \quad \hat{K}_N^{(1)} = \frac{1}{N} \sum_{n=1}^N \hat{K}_N^{(1, \setminus n)} = J - \frac{f_{N,1}}{N}. \quad (43)$$

Therefore, the order 1 jackknife estimator for the total population size is obtained by plugging in $\hat{\psi}_N^{(0)} = J$ and $\hat{\psi}_N^{(1)} = J - \frac{f_{N,1}}{N}$ in Equation (41):

$$\hat{K}_N^{J_1} = J + \frac{N-1}{N} f_{N,1} \quad (44)$$

The case for general p : For any $p \leq N$, it always holds that

$$\hat{K}_N^{(p)} = J - \binom{N}{p}^{-1} \sum_{\ell=1}^p \binom{N-\ell}{p-\ell} f_{N,\ell} \quad (45)$$

This formula allows to obtain the general Jackknife estimator of order p , which is a linear function of the observed number of species J and correction terms which depend on the fingerprint f_N ,

$$\hat{K}_N^{J_p} = \sum_{\ell=1}^p a_{N,\ell}^{(p)} f_{N,\ell}.$$

D.2 Estimators for the number of hitherto unseen genomic variants

Taking inspiration from the approach of Burnham and Overton [1978], Gravel et al. [2011] and Gravel [2014] developed Jackknife estimators for the number of hitherto genomic variants which are going to be observed in M additional samples given N initial ones. Let $V(N)$ denote the total number of variants observed in N samples, and let $\Delta(N+M, N) := H_{N+M-1} - H_{N-1} = \sum_{\ell=N}^{M+N-1} 1/\ell$, where

$$H_N = 1 + 1/2 + \dots + 1/N$$

is the N -th harmonic number. To derive their estimators, the authors use the assumption that for a given order $p \geq 1$ the total number of variants present in $N+M$ samples can be estimated as follows:

$$\hat{V}_N^{(M)} = V(N) + \sum_{\ell=1}^p a_{N,\ell}^{(p)} \Delta(N+M, N)^\ell, \quad (46)$$

where $\mathbf{a}_N^{(p)} = [a_{N,1}^{(p)}, \dots, a_{N,p}^{(p)}]$ are constants which depend on the initial sample size N , on the order p and on the fingerprint of the sample \mathbf{f}_N . This assumption is exact in the case of a constant size and neutrally evolving population (Gravel et al. [2011]). For a given order p the unknown coefficients are obtained by solving the following system of equations:

$$\hat{V}_N^{(M)} = \hat{V}_{N-1}^{(M)} = \dots = \hat{V}_{N-p}^{(M)}. \quad (47)$$

Equating $\hat{V}_N^{(M)}$ to $\hat{V}_{N-j}^{(M)}$ using Equation (46) for $j = 1, \dots, p$, we obtain a system of $p - 1$ equations of the form

$$V(N) - V(N - j) = \sum_{\ell=1}^p a_{N,\ell}^{(p)} (\Delta(N + M, N - j)^\ell - \Delta(N + M, N)^\ell). \quad (48)$$

Using the additional equality

$$V(N) - V(N - \ell) = \sum_{j=1}^{\ell} \frac{\binom{\ell}{j}}{\binom{N}{j}} f_{N,j}. \quad (49)$$

we can solve for $a_{N,\ell}^{(p)}$ and express these in terms of N , $\Delta(N + M, N)$ and the fingerprint \mathbf{f}_N , and the final estimator is a linear function of the fingerprint \mathbf{f}_N .

D.3 Choice of the jackknife order

As pointed out in Burnham and Overton [1978], the optimal order p of the jackknife estimator heavily depends on the data under consideration. It is therefore desirable to obtain a procedure which uses the data to guide the choice of such order. Burnham and Overton [1978] phrase this decision problem as a sequential hypothesis test, in which one keeps increasing the order of the jackknife until the data suggests that the drop in bias obtained by increase the jackknife order is exceeded by the gain in variance. Precisely, for $p = 1, 2, \dots$ one sequentially performs the following test:

$$H_{0,p} : \mathbb{E}(\hat{K}_N^{J_{p+1}} - \hat{K}_N^{J_p}) = 0 \quad \text{versus} \quad H_{a,p} : \mathbb{E}(\hat{K}_N^{J_{p+1}} - \hat{K}_N^{J_p}) \neq 0. \quad (50)$$

If $H_{0,p}$ is rejected, this has to be interpreted as evidence that the bias reduction provided by the $p + 1$ -th order (with respect to the p -th) is larger than the associated increase in variance, and $p + 1$ -th order should be preferred to the p -th order [Burnham and Overton, 1978]. The first order p for which the test fails to reject the null hypothesis is chosen as the jackknife order.

The test relies on the following observation: the difference between two jackknife estimators of different orders $p + 1$ and p is given by

$$\hat{K}_N^{J_{p+1}} - \hat{K}_N^{J_p} = \sum_{\ell=1}^{p+1} \tilde{a}_{N,\ell}^{(p+1,p)} f_{N,p}, \quad (51)$$

again a linear combination of the fingerprint. Because the conditional distribution of the fingerprint is independent of K given J , the minimum variance estimator of the conditional variance is given by

$$\text{est var}(\hat{K}_N^{J_{p+1}} - \hat{K}_N^{J_p} | J) = \frac{J}{J-1} \left\{ \sum_{\ell=1}^p (\tilde{a}_{N,\ell}^{(p+1,p)})^2 f_{N,\ell} \frac{(\hat{K}_N^{J_{p+1}} - \hat{K}_N^{J_p})^2}{J} \right\}. \quad (52)$$

Under $H_{0,p}$, the test statistic

$$T_p = \frac{\hat{K}_N^{J_{p+1}} - \hat{K}_N^{J_p}}{\sqrt{\text{est var}(\hat{K}_N^{J_{p+1}} - \hat{K}_N^{J_p} | J)}} \quad (53)$$

is approximately normally distributed.

For a given extrapolation size M , we can apply the same procedure to the estimators derived in Gravel et al. [2011] and Gravel [2014], which are again linear combinations of the fingerprint.

E Good-Toulmin estimators

In recent work, Chakraborty et al. [2019] used the classic smoothed Good-Toulmin estimator [Good and Toulmin, 1956, Efron and Thisted, 1976, Orlitsky et al., 2016] in the context of rare variants prediction. Under the same sampling model assumed by Zou et al. [2016], this method allows to predict the number of additional variants that will be observed in M additional samples by using the formula

$$\Delta_N(M) | X_{1:N} = \begin{cases} \sum_{r=1}^{\infty} (-1)^{r+1} \left(\frac{M}{N}\right)^r f_r & \text{if } M/N \leq 1 \\ \sum_{r=1}^{\infty} (-1)^{r+1} \left(\frac{M}{N}\right)^r f_r P(M, N, r) & \text{if } M/N > 1 \end{cases}, \quad (54)$$

where

$$P(M, N, r) = \Pr(\text{Binomial}(\kappa(M, N), \theta(M, N)) \geq r) \quad (55)$$

where the smoothing parameters κ and θ can take two different forms: either

$$\kappa(M, N) = \lfloor 0.5 \log_2((M^2/N)/(M/N - 1)) \rfloor \quad \text{and} \quad \theta(M, N) = 1/(M/N + 1)$$

or

$$\kappa(M, N) = \lfloor 0.5 \log_3((M^2/N)/(M/N - 1)) \rfloor \quad \text{and} \quad \theta(M, N) = 2/(M/N + 2).$$

F Additional experimental results

F.1 Further details on data and experimental setup

In order to run our experiments, we use data from the gnomAD (genome aggregation dataset) discovery project [Karczewski et al., 2019], the largest and most comprehensive publicly available human genome dataset. This dataset contains 125'748

exomes sequences (i.e. protein-coding regions of the genome), from 8 main populations (African American, Latino, Ashkenazi Jewish, East Asian, Finnish, Non-Finnish European, South Asian, Other¹). Sample size varies widely across sub populations, e.g. the “Other” subgroup counts only 3’070 observations, while “Non-Finnish European” contains 56’885 individuals. Moreover, some of these main populations are further split into additional sub populations, e.g. “Non-Finnish European” contains the “Bulgarian”, “Estonian”, “Northern European”, “Southern European”, “Swedish”, “Other European” sub populations, while the “East Asian” sub population is further split into the “Korean”, “Japanese” and “Other East Asian” sub populations (see Karczewski et al. [2019] for additional details). We ran our analysis on all populations and sub populations.

Because for privacy reasons not all individual sequences are accessible, in order to run our analysis we generate synthetic data which closely resembles the true data as follows. For every subpopulation with N individuals and every position $j = 1, \dots, K$ in the exome, we have access to the total number of individuals N_j showing variation at position j . We compute the empirical frequency of variation at site j , $\hat{\theta}_j := N_j/N$ for all $j = 1, \dots, K$. Our data is then generated by sampling independent Bernoulli random vectors X_1, \dots, X_N , with $X_n = [x_{n,1}, \dots, x_{n,K}]$. The entries in the vector are independent Bernoulli random variables, $x_{n,j} \sim \text{Bernoulli}(\hat{\theta}_j)$.

For the optimal design experiments, i.e. in the setting in which samples are noisy, we perform further thinning to generate the data. That is to say, given the empirical frequencies $\{\hat{\theta}_j\}$, $j = 1, \dots, K$ and for a given choice of T , sampling error p_{err} and sequencing quality λ , we obtain the associated probability ϕ that at least T successful reads are obtained at any position j for any individual n , i.e.

$$\phi(\lambda, T, p_{\text{err}}) := \sum_{t \geq T} \frac{1}{t!} e^{-\lambda(1-p_{\text{err}})} \{\lambda(1-p_{\text{err}})\}^t.$$

Then, an individual observation $X_n = [x_{n,1}, \dots, x_{n,K}]$ is obtained by independently sampling Bernoulli random variables,

$$x_{n,j} \mid \hat{\theta}_j, \phi(\lambda, T, p_{\text{err}}) \sim \text{Bernoulli}(\hat{\theta}_j \phi(\lambda, T, p_{\text{err}})).$$

F.2 Synthetic data from the Indian buffet process

In this section, we provide experimental results for data drawn from the three parameters Indian buffet process. When the data is drawn from the true model, we expect the Bayesian nonparametric estimators of Section 3 to work particularly well. We test against a large collection of parameters $\alpha > 0$, $\sigma \in [0, 1]$ and $c > -\sigma$. We report here results for different configurations. In all cases, the optimization procedure outlined in Section 6 recovers the rate of growth of the distinct variants. Interestingly, in some instances, the optimization recovers parameters that differ from the true parameters that generate the process, but still have good predictive performance (see Figure 4).

¹The “Other” subgroup contains all “individuals were classified as ”other” if they did not unambiguously cluster with the major populations in a principal component analysis”

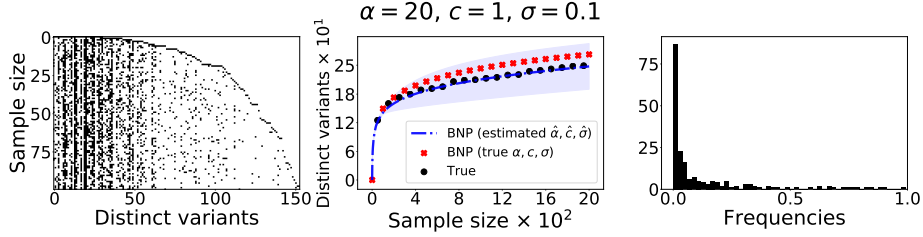


Figure 4: A draw from a three-parameter Indian buffet process. Here, $\alpha = 20$, $c = 1$, $\sigma = 0.1$. In the left panel, we see the binary matrix \mathbf{X} containing the first $N = 100$ samples (x -axis) from the process, in its left-ordered-form (lof) – i.e. variants (y -axis) are sorted by the order of appearance, so that as more points are added to the dataset, more columns contain nonzero entries. In the central panel, we plot the number of distinct variants (y -axis) as a function of the sample size (x -axis), extrapolating up to $M = 1900$ additional samples. Last, on the right panel, we plot the empirical distribution of frequencies among the first N samples.

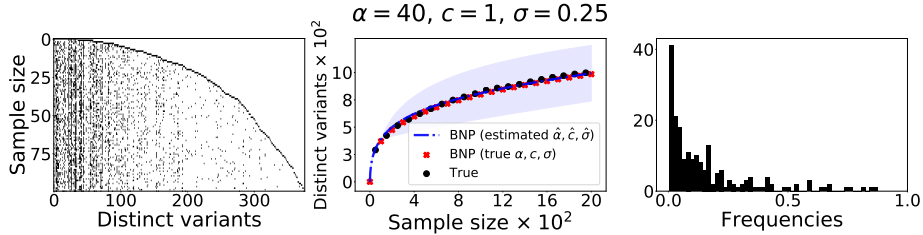


Figure 5: In this figure, we reproduce the visualizations explained in Figure 4 for a draw from a three-parameter Indian buffet process with parameters $\alpha = 40$, $c = 1$ and $\sigma = 0.25$

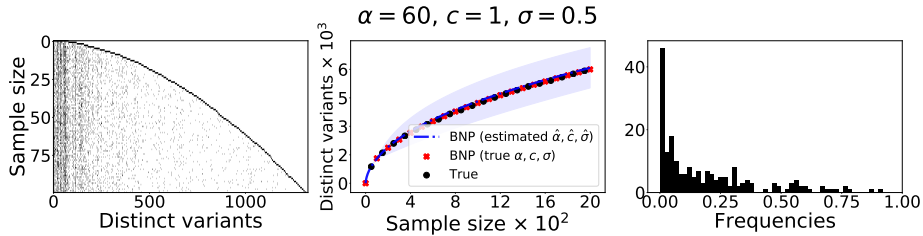


Figure 6: In this figure, we reproduce the visualizations explained in Figure 4 for a draw from a three-parameter Indian buffet process with parameters $\alpha = 60$, $c = 1$ and $\sigma = 0.5$

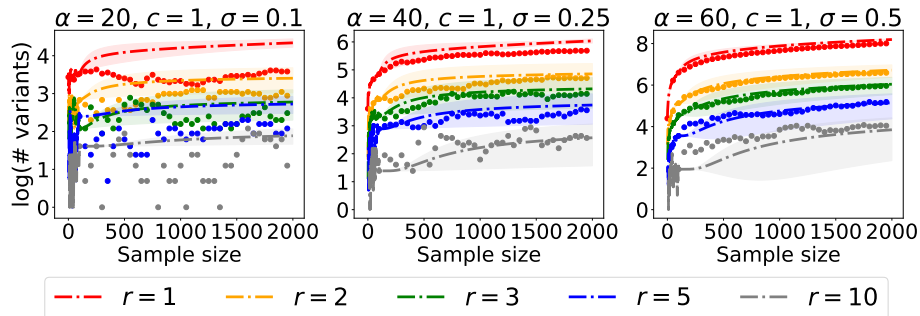


Figure 7: In this figure, for the three configurations of parameters α, c, σ considered in Figure 4, Figure 5 and Figure 6, we plot the performance of the estimators $P_N^{(M,r)}$ for $M = 1, \dots, 1900$ and $r = 1, 2, 3, 5, 10$. Dotted line show the performance of the estimators, while points show the true values of the process.

We also tested the performance of the predictor $P_N^{(M,r)}$ for the number of new variants that are going to appear a given number r of times as the initial sample of size N is enlarged with M additional observations. We found the performance of the predictor, in this case, to be very sensitive to the value of σ . In particular, while we expect the estimator to be exact as the extrapolation size M diverges, we observe that when σ is close to 0, the performance degrades for small values of r .

F.3 Synthetic data from the beta-Bernoulli model

Ionita-Laza et al. [2009] under the true model: We first consider the case in which the variants frequencies $\theta_1, \dots, \theta_K$ are independently and identically distributed draws from a beta distribution, i.e. for some parameters $\alpha > 0$ and $\beta > 0$, independently and identically distributed across $j = 1, \dots, K$ it holds

$$\theta_j \sim f(\theta) \propto \theta^{\alpha-1} (1-\theta)^{\beta-1} \mathbf{1}_{(0,1)}(\theta). \quad (56)$$

Conditionally on the variants $\theta_1, \dots, \theta_K$, each observation X_n is a binary vector of independent Bernoulli random variables, $x_{n,j} \mid \theta_j \sim \text{Bernoulli}(\theta_j)$. This is exactly the model considered by Ionita-Laza et al. [2009]. Therefore we are not surprised to verify in Figure 8 that the predictor derived in Appendix B outperforms the Bayesian nonparametric counterpart when the variants comes from the model of Equation (56).

Ionita-Laza et al. [2009] under misspecification: the case of power laws: Here we consider the case in which the variants frequencies $\theta_1, \dots, \theta_K$ are independently and identically distributed draws from a power law distribution, i.e. for some tail exponent $\xi \geq 0$

$$\theta_j \sim f(\theta) \propto \theta^{-\xi} \mathbf{1}_{(0,1)}(\theta). \quad (57)$$

The parameter ξ controls the left tail of the distribution: for $\xi = 0$, the distribution is uniform over the support $[0, 1]$. The larger the value of ξ , the more mass we put over

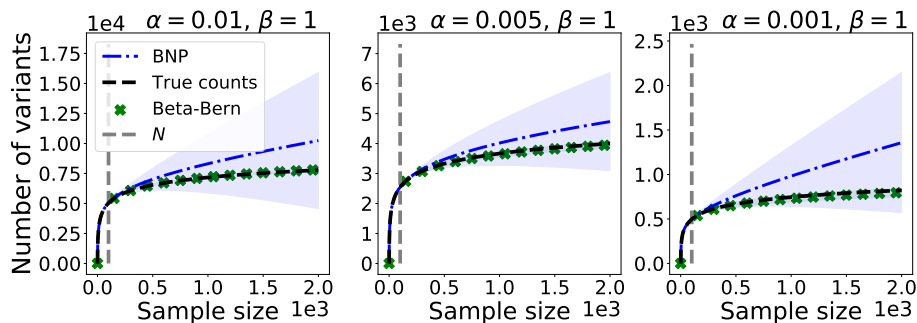


Figure 8: Performance of the beta-Bernoulli predictor (green crosses) proposed by Ionita-Laza et al. [2009] and of the nonparametric Bayesian predictor (dotted blue line) on three different datasets (each panel represents a different dataset). Each dataset is generated as follows: we first draw a random vector θ of dimension $K = 10^4$. The K coordinates are independently and identically distributed draws from a beta distribution. Conditionally on θ , we draw a random matrix \mathbf{X} with $N = 2000$ rows and K columns. The (n, j) -th entry $x_{n,j}$ is Bernoulli distributed with mean θ_j , so that the columns of \mathbf{X} are independently and identically distributed. We retain the first $N = 200$ rows as training set and obtain the two estimators. We project up to $N + M = 2000$ observations. We repeat the procedure over ten distinct folds of the data of the same size N to produce estimates of the prediction error. These estimate of the error is displayed by plotting one empirical standard deviation across the ten predicted values across the different folds, for each extrapolation value $\ell = 201, \dots, 2000$. From left to right, we vary the first shape parameter of the beta distribution $\alpha \in \{10^{-1}, 10^{-2}, 10^{-2} \times 2^{-1}\}$, driving the mean of the distribution to zero, while keeping the second parameter $\beta = 1$ fixed.

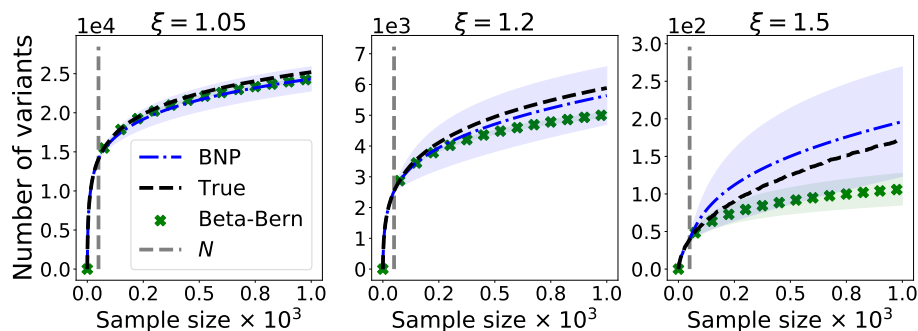


Figure 9: Performance of the beta-Bernoulli predictor (green solid line) proposed by Ionita-Laza et al. [2009] versus the nonparametric Bayesian predictor (dotted blue line) on three different datasets (each panel represents a different dataset). Each dataset is generated as follows: we first draw a random vector θ of dimensions $K = 10^4$. The K coordinates are independently and identically distributed draws from a power law distribution as described in Equation (57). Conditionally on θ , we draw a random matrix X with $N = 1000$ rows and K columns. The (n, j) -th entry $x_{n,j}$ is Bernoulli distributed with mean θ_j , so that the columns of X are independently and identically distributed. We retain the first $N = 50$ rows as training set and obtain the two predictors. We project up to $N + M = 1000$ observations. We repeat the procedure over ten folds of the same data of same size $N = 50$. We repeat the procedure over ten folds of the same data to produce estimates of the prediction error. These estimate of the error is displayed by plotting one empirical standard deviation across the ten predicted values across the different folds, for each extrapolation value $\ell = 51, \dots, 1000$. From left to right, we vary the exponent of the power law distribution (left, $\xi = 1.05$, center, $\xi = 1.2$, right $\xi = 1.5$).

rare frequencies. Power laws arise in a vast number of natural phenomena, including ecology, biology, physical and social sciences [Clauset et al., 2009]. Therefore, having an estimator that is effective when frequencies exhibit a power law behavior is desirable for virtually any applied scenario. In our experiments, the Bayesian parametric approach works well for moderate exponents, i.e. when the power law behavior is relatively mild. However, as soon as the exponent ξ becomes large, the parametric model fails to deliver consistent results (see Figure 9). Conversely, the Bayesian nonparametric estimator performs reasonably well.

F.4 The choice of the hyperparameter κ for the frequentist non-parametric estimator proposed by Zou et al. [2016]

Choosing the parameter κ is particularly challenging when the sample size N is small relative to the total number of frequencies - as in the genomics application we consider. As a general principle, in order to avoid numerical instability, the input size has to be sufficiently large. For example, given a sample of $N = 100$ observations, if one sets $\kappa = 1$, the algorithm will take as an input only the number of variants which have

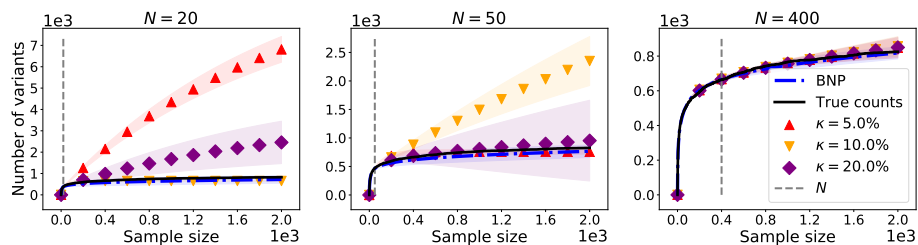


Figure 10: Comparison of the Bayesian nonparametric estimator (blue dotted line) to the frequentist nonparametric estimator proposed by Zou et al. [2016]. We generate synthetic datasets as follows: we first draw a random vector θ of $K = 10^4$ independently and identically distributed beta random variables with parameters $\alpha = 0.001$ and $\beta = 1$. Conditionally on θ , we draw a random matrix X with $N = 2000$ rows and K columns. In each subplot, we retain a different fraction of rows of X to be used as training set (from left to right, $N \in \{20, 50, 400\}$). For each value of N , we compute the Bayesian nonparametric estimator, as well as the frequentist nonparametric estimator, varying the threshold parameter $\kappa \in \{5\%, 10\%, 20\%\}$ (red (+), orange (*), purple (\diamond)) respectively. We highlight how the performance of the frequentist nonparametric estimator, especially when N is small, highly depends on the choice of κ , in an counterintuitive and somewhat unpredictable way. For example, when $N = 20$, choosing $\kappa = 10\%$ provides much better results than $\kappa = 5\%$ or $\kappa = 20\%$. However, for $N = 50$, both $\kappa = 5\%$ and $\kappa = 20\%$ perform much better than $\kappa = 10\%$. As N increases, the performance of the nonparametric frequentist estimator stabilizes, and becomes less sensitive to the choice of the parameter κ .

been observed once. This will typically lead to numerical instability, which will not arise for larger values of κ (e.g. $\kappa \geq 10$). A general rule of thumb one could follow is to decrease κ as a function of the training sample size N : the larger N , the smaller κ . While this intuition seems to work on some instances, we found cases in which unpredictable behaviors can affect the quality of the predictions (see Figure 10 and Figure 11).

F.5 Bias variance tradeoff for the Jackknife estimator and optimal choice of the order p

As discussed in Burnham and Overton [1978], Gravel et al. [2011], Gravel [2014], and briefly in Appendix D.3, the prediction quality of jackknife estimators crucially depends on the *order* chosen. Lower orders can suffer from large bias, but have small variance, while higher orders incur in less bias at the cost of higher variance. On different datasets, the accuracy of different orders can vary dramatically. In this section we provide some experimental results (see Figure 12) to illustrate this tradeoff.

In this section we provide some experimental results (see Figure 12) to illustrate this tradeoff.

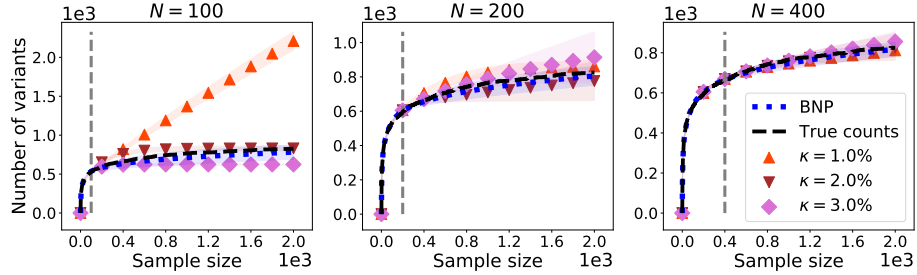


Figure 11: Comparison of the Bayesian nonparametric estimator (blue dotted line) to the frequentist nonparametric estimator of Zou et al. [2016]. We use the same data showed in Figure 10 but using much smaller values of $\kappa \in \{1\%, 2\%, 3\%\}$. Trying to run the linear program for these values of κ and $N < 100$ causes issues in the optimization routine, and therefore we only test it for N sufficiently large. We notice that for both $N = 100$ and $N = 200$, the suggested value of $\kappa = 1\%$ provides worse results than choosing a larger value of κ , whereas for $N = 400$, the performance of the estimator becomes less sensitive to the choice of κ .

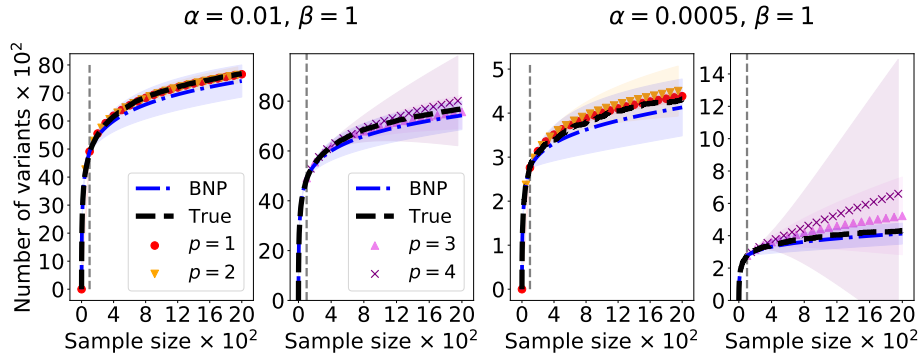


Figure 12: Comparison of the Bayesian nonparametric estimator (blue dotted line) to the jackknife estimator of Gravel [2014] for different choices of the order p . We generate two datasets as follows: for $\alpha \in \{0.01, 0.0005\}$ and $\beta = 1$, we generate two sets of $K = 10^4$ independently and identically distributed beta distributed draws θ with parameters α, β . We then draw a random matrix \mathbf{X} with $N = 2000$ rows, in which each entry $x_{n,j}$ is Bernoulli distributed with mean θ_j . We retain $N = 100$ rows for training. The two left panels show results for the dataset obtained when $\alpha = 0.01, \beta = 1$ across different choices of the jackknife order p . The two right panels show the same results for the dataset obtained when $\alpha = 0.0005$. Lower order jackknife estimators perform extremely well, and have little variance, while higher order jackknife estimators have worse performance, and higher variance. Such behavior worsens as α gets smaller, i.e. when the mean of the beta draws approach 0.

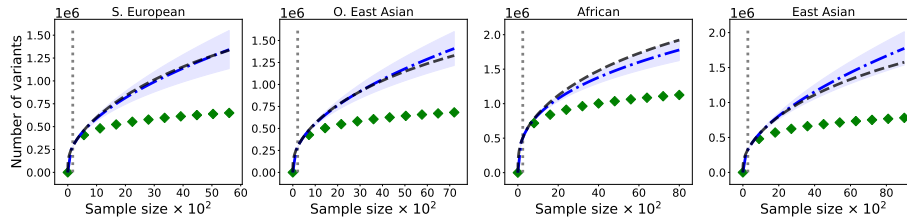


Figure 13: The blue dotted line is the posterior predictive mean of the number of distinct variants $U_N^{(m)}$ observed according to the Bayesian nonparametric predictor, averaged across 33 samples of size N . The green diamonds report the posterior predictive mean of the Bayesian parametric estimator of Ionita-Laza et al. [2009], averaged across the same subsets of the original data. The shaded blue and green regions report the prediction error by covering one standard empirical deviation for the two predictors.

F.6 Additional plots from the gnomAD project

In Figure 13, Figure 14 and Figure 15 we report results of the prediction of the number of new variants on some sub populations of the gnomAD dataset. We consider the Bulgarian, South Korean, Other East Asian, African and East Asian subpopulations. The x -axis displays the total number of samples collected. On the y -axis, we plot the number of distinct genomic variants. The solid black line displays the true number of distinct variants, the vertical grey line is placed in correspondence of the training sample size N (left: $N \in \{42, 61, 228, 257, 291\}$).

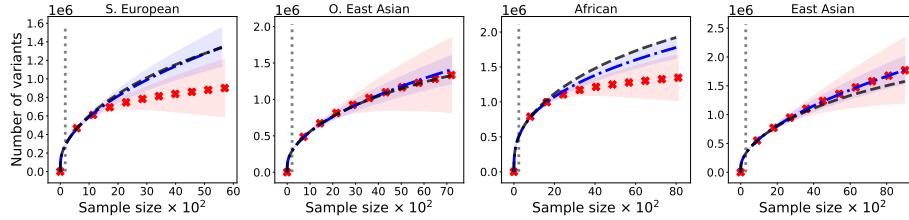


Figure 14: Results of the estimation of the number of new variants on some sub populations of the gnomAD dataset. The x -axis displays the total number of samples collected. On the y -axis, we plot the number of distinct genomic variants observed. The solid black line keeps track of the true number of distinct variants, the vertical grey line is placed in correspondence of the training sample size N . The blue dotted line is the posterior predictive mean of the number of distinct variants $U_N^{(m)}$ observed according to the Bayesian nonparametric predictor, averaged across 33 samples of size N . The dotted red line is the empirical mean of the UnseenEST estimator of Zou et al. [2016] across the same samples. The shaded blue and red regions report the prediction error by covering one standard empirical deviation for the two predictors. Here, we fix $\kappa = 1\%$, the value considered in Zou et al. [2016].

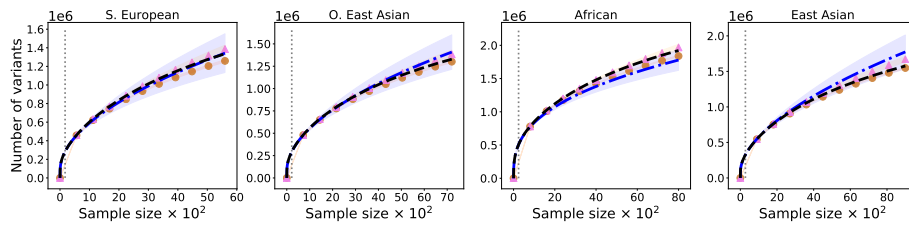


Figure 15: Again for the same sub populations considered in Figure 13 and Figure 14, we compare the Bayesian nonparametric estimator to the Jackknife estimator proposed in Gravel [2014], for the third and fourth orders. Lower order consistently underestimate the number of distinct variants

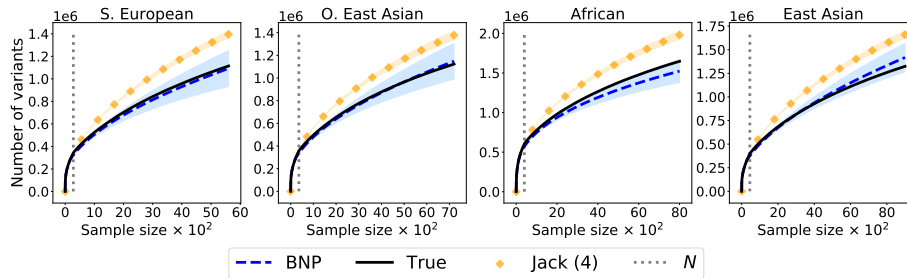


Figure 16: Prediction of the number of yet unseen variants for five subpopulations (gnomAD). For each subpopulation, we assume to have access to a small number of high quality genetic samples N in which variation is observed at J distinct loci, collected at initial sequencing depth $\lambda_{\text{pilot}} = 45$ and threshold $T = 30$. We imagine that the follow-up is performed at a different sequencing depth, $\lambda_{\text{follow}} = 32$.